FTD-HT-23-1510-68

FOREIGN TECHNOLOGY DIVISION

ATMOSPHERIC TURBULENCE AND RADIO WAVE PROPAGATION

(SELECTED ARTICLES)

76

FTD-HT-23-1510-68

EDITED TRANSLATION

ATMOSPHERIC TURBULENCE AND RADIO WAVE PROPAGATION
(SELECTED ARTICLES)

English pages: 70

SOURCE: Atmosfernaya Turbulentnost' I Rasprostraneniye Radiovoln. Trudy, 1967, pp. 30-52, 76-92, 179-190.

Translated by: Contract F33657-68-D-0866 P002

PREPARED BY:

TRANSLATION DIVISION
FOREIGN TECHNOLOGY DIVISION
WP-AFB, OHIO.

Date 13 May 19 69

DATA HANDLING PAGE

01-ACCESSION NO. 98-DOCUMENT LOC	39-TOPIC TAGS
TT9000675	atmospheric turbulence, meteorology, statistic analysis
09-TITLE EMPIRICAL DATA ON THE SMALL-SCALE STRUCTURE OF ATMOSPHERIC TURBULENCE	
47-SUBJECT AREA 04	

12-AUTHOR/CO-AUTHORS	10-DATE OF INFO
GURVICH, A. S.;16-KOPROV, B. M.;16-TSVANG, L. R.;16-YAGLOM, A. M.	-----67
13-SOURCE ATMOSFERNAYA TURBULENTNOST' I RASPROSTRANENIYE RADIOVOLN. TRUDY MOSCOW IZD-VO "NAUKA" (RUSSIAN) FTD-	68-DOCUMENT NO. HT-23-1510-68
	69-PROJECT NO. 72301-78

63-SECURITY AND DOWNGRADING INFORMATION	64-CONTROL MARKINGS	97-HEADER CLASN
UNCL, 0	NONE	UNCL

76-REEL FRAME NO.	77-SUPERSEDES	78-CHANGES	40-GEOGRAPHICAL AREA	NO OF PAGES
1888 1905			UR	31

CONTRACT NO.	X REF ACC. NO.	PUBLISHING DATE	TYPE PRODUCT	REVISION FREQ
F33657-68-D 0866 P002	65-AT8005282	94-00	TRANSLATION	NONE

STEP NO.	ACCESSION NO.
02-UR/0000/67/000/000/0030/0052	

ABSTRACT

(U) The published literature on small-scale atmospheric turbulence is surveyed and statistical methods for processing empirical data are discussed. The survey covers the following topics: 1) The spectra and structural functions of meteorological fields; 2) Taylor's hypothesis on "frozen turbulence"; 3) Inertial interval of the turbulence spectrum; 4) The effect of molecular viscosity and heat conductivity on the spectra of meteorological fields; and 5) The characteristics of non-isotropic turbulence perturbations. Principle attention is devoted to the double-point second order moments. Another general method for obtaining small-scale characteristics involves the use of Fourier transformations and the consideration of statistical quantities which depend only on spectral components with large frequencies or large wave numbers. The theoretical disavantages of measuring time spectra are discussed. The application of Taylor's hypothesis concerning "frozen" patterns of turbulence to obtain space characteristics from time characteristics is also discussed. Experimental work conducted at the field station of the Institute for the Physics of the Atmosphere have shown that Taylor's hypothesis can be applied over a greater range than initially anticipated. Methods of collecting observed data are discussed. Methods of determining numerical coefficients in the "2/3 law" and the "5/3 law" for temperature and for other scalar quantities are reviewed. Orig. art. has: 19 formulas, 6 figures.

DATA HANDLING PAGE

01-ACCESSION NO. 98-DOCUMENT LOC TT9000676	39-TOPIC TAGS atmospheric turbulence, wind velocity, atmospheric temperature, meteorologic tower, surface boundary layer
09-TITLE TURBULENCE CHARACTERISTICS OF WIND SPEED AND TEMPERATURE IN THE BOUNDARY LAYER OF THE ATMOSPHERE	
47-SUBJECT AREA 04	

12-AUTHOR/CO-AUTHORS BYZOVA, N. L. ; 16-IVANOV, V. N.; 16-MOROZOV, S. A.	10-DATE OF INFO -----67
43-SOURCE ATMOSFERNAYA TURBULENTNOST' I RASPROSTRANENIYE RADIOVOLN. TRUDY MOSCOW IZD-VO "NAUKA" (RUSSIAN) FTD-	68-DOCUMENT NO. HT-23-1510-68
	69-PROJECT NO. 72301-78

63-SECURITY AND DOWNGRADING INFORMATION UNCL, 0			64-CONTROL MARKINGS NONE	97-HEADER CLASN UNCL
76-REEL FRAME NO. 1888 1906	77-SUPERSEDES	78-CHANGES	40-GEOGRAPHICAL AREA UR	NO OF PAGES 22
CONTRACT NO. F33657-68-D-0866 P002	X REF ACC. NO. 65-AT8005283	PUBLISHING DATE 94-00	TYPE PRODUCT TRANSLATION	REVISION FREQ NONE
STEP NO. 02-UR/0000/67/000/000/0076/0092			ACCESSION NO.	

ABSTRACT (U) Experimental investigations of wind velocity and temperature carried out with the aid of the 300 meter meteorological tower of the Institute of Applied Geophysics are described. The following topics are covered: 1) wind velocity spectra in the infrasonic frequency range, 2) turbulent energy of the longitudinal wind velocity component; 3) large scale heterogeneities; 4) dissipation of turbulent energy; 5) variation in the intensity of temperature heterogeneities as a function of time; 6) variation in the intensity of temperature heterogeneities as a function of altitude. The computer-calculated spectral density of the longitudinal wind velocity component is shown in Fig. 1. This figure shows that the energy distribution in the considered range of frequencies has a sharply defined minimum which separates the turbulent and mesometeorological region of the spectrum. At the lower levels the minimum has a frequency of 0.15-4 cycles/hr while at the upper levels this frequency is 0.15-2 cycles/hr. The results also confirm the existence of a half-day maximum which coincides with results reported elsewhere. The turbulent energy was evaluated for the frequency range of from 0.5 cycles/sec up to 2 cycle/hr. Fig. 2 shows the longitudinal turbulence intensity as a function of the time of day and altitude. Fig. 3 shows the variation in the intensity of turbulence as a function of altitude for different stratification. Orig. art. has: 17 figures, 6 formulas.

DATA HANDLING PAGE

01-ACCESSION NO. 98-DOCUMENT LOC TT9000677	39-TOPIC TAGS atmospheric turbulence, planetary boundary layer, atmospheric stratification, jet stream, atmospheric radiation
09-TITLE TURBULENT EXCHANGE IN THE THERMALLY STRATIFIED PLANETARY BOUNDARY LAYER OF THE ATMOSPHERE	
47-SUBJECT AREA 04	

12-AUTHOR CO-AUTHORS BOBYLEVA I. M.;16-ZILITINKEVICH, S. S. ; 16-LAYKHTMAN, D. L.	10-DATE OF INFO -----67
63-SOURCE ATMOSFERNAYA TURBULENTNOST' I RASPROSTRANENIYE RADIOVOLN. TRUDY MOSCOW IZD-VO "NAUKA" (RUSSIAN) FTD-HT-23-1510-68	68-DOCUMENT NO. HT-23-1510-68 69-PROJECT NO. 72301-78

63-SECURITY AND DOWNGRADING INFORMATION UNCL, 0			64-CONTROL MARKINGS NONE	97-HEADER CLASN UNCL
76-REEL FRAME NO. 1888 1907	77-SUPERSEDES	78-CHANGES	40-GEOGRAPHICAL AREA UR	NO OF PAGES 17
CONTRACT NO. F33657-68-D-0866 P002	X REF ACC. NO. 65-AT8005285	PUBLISHING DATE 94-00	TYPE PRODUCT TRANSLATION	REVISION FREQ NONE
STEP NO. 02-UR/0000/67/000/000/0179/0190			ACCESSION NO.	

ABSTRACT
(U) The turbulent state of the thermally stratified planetary boundary layer is analyzed, assuming that the effect of radiation heat transfer is negligibly small. The system of equations for turbulent motion based on the semi-empirical theory is given. Appropriate boundary conditions are determined when the problem is expressed in terms of a set of universal functions of variables which depend on the parameter. The problem was solved numerically on the M-20 digital computer. The following results are plotted and discussed: variation in the geostrophic coefficient of friction as a function of the Rossby number; variation in the angle of complete wind reversal in the boundary layer as a function of the Rossby number; universal profiles for the coefficient of turbulent viscosity; universal profiles for the rate of turbulent energy dissipation; universal profiles of the wind in the boundary layer. The thickness of the "jet stream" turns out to be several tens of meters and the maximum velocity is 1.5 times greater than the geostrophic value. The authors express their gratitude to G. I. Marchuk for valuable discussions. Orig. art. has: 6 figures, 31 formulas.

TABLE OF CONTENTS

BLANK PAGE

EMPIRICAL DATA ON THE SMALL-SCALE STRUCTURE OF ATMOSPHERIC TURBULENCE

A.S. Gurvich, B.M. Koprov,
L.P. Tsvang and A.M. Yaglom

Institute of Atmospheric Physics of the
USSR Academy of Sciences
Moscow, USSR

1. SPECTRA AND STRUCTURAL FUNCTIONS OF THE METEOROLOGICAL FIELDS

Turbulent motion is characterized by the presence of disordered pulsations of all meteorological fields and admits only of statistical description. As we know, complete description of this type requires assignment of all multidimensional probability distributions for the values of all possible hydrodynamic fields at various populations of the points (x,t) in four-dimensional space-time (see, for example, [1], §3). However, it is a very difficult task to determine even a uniform probability distribution from empirical data; finding multidimensional distributions is, of course, many times more complex. Hence the overwhelming majority of empirical investigations in the field of turbulence have not been devoted to study of the probability distributions themselves, but to study of only certain of their simplest numerical characteristics. Since the moments of the distribution are at the same time the most important and the simplest of its numerical characteristics, it is surprising that almost all of the information presently available on atmospheric turbulence is concerned with various moments of the meteorological fields. Invariably, only single-point or

double-point moments are considered, i.e., averages of the products of the values of meteorological fields at one or at most two different points in space-time. We also shall examine only certain single-point and double-point moments, concentrating our attention on double-point moments, which permit substantially simpler derivation of characteristics that depend only on the small-scale turbulence components.

Double-point moments of the second order are the most important. The most general moment of this type is the space-time cross-correlation function of two meteorological fields a(x,t) and b (x,t) which is given by the formula

$$B_{ab}(\mathbf{x}, \mathbf{r}, t, \tau) = \overline{a(\mathbf{x}+\mathbf{r}, t+\tau)\, b(\mathbf{x}, t)} \tag{1}$$

(here and consistently in this paper, the overbar denotes averaging, understood in the conventional probability-theory sense). However, cross-correlation functions are inconvenient in that they are determined basically by turbulence components of relatively large scale. The simplest way to isolate the contribution of small-scale pulsations is to convert, following Kolmogorov [2], to a coordinate system that moves together with a fixed liquid particle and examine, instead of the actual meteorological-field values, the differences between these values at relatively proximate space-time points. If we limit ourselves to purely spatial characteristics only (characteristics pertaining to a fixed time t), this approach results in substitution of the space cross-correlation functions by simple linear combinations of these functions – the cross structure functions

$$D_{ab}(\mathbf{x}, \mathbf{r}, t) = \overline{[a(\mathbf{x}+\mathbf{r}, t) - a(\mathbf{x}, t)]\,[b(\mathbf{x}+\mathbf{r}, t, - b(\mathbf{x}, t)]}. \tag{2}$$

The space structure functions of one field represent a particular case of the functions (2):

$$D_{aa}(\mathbf{x}, \mathbf{r}, t) = \overline{[a(\mathbf{x}+\mathbf{r}, t) - a(\mathbf{x}, t)]^2}. \tag{3}$$

Another general method for isolation of local turbulence characteristics consists in the use of Fourier transforms and analysis of statistical quantities that depend only on spectral components with high frequencies or wave numbers. The general space-time cross spectrum of the fields a(x,t) and b(x,t) can be determined as the four-dimensional Fourier transform of correlation function (1) with respect to the variables r and τ:

$$F_{ab}(\mathbf{k}, \omega) = \frac{1}{(2\pi)^4} \int e^{-i(\mathbf{kr}+\omega\tau)} B_{ab}(\mathbf{r}, \tau)\, d\mathbf{r}\, d\tau, \tag{4}$$

where integration extends over the entire four-dimensional space r,τ (we shall not indicate the dependence of the functions B_{ab} and F_{ab} on x and t explicitly at this time). In the important case of uniform and stationary fields, when Function (1) is totally independent of the variables x and t, the quantity $F_{ab}(\mathbf{k}, \omega)\, d\mathbf{k} d\omega$ can be interpreted as the average product of the

Fourier component of field $a(x,t)$ that corresponds to volume element $dkd\omega$ of field (k,ω) by the complex-conjugate value of the analogous Fourier component of field $b(x,t)$ (see, for example, [3-5]). From this, among other things, it follows that the spectrum $F_{aa}(k,\omega)$ of the homogeneous field $a(x,t)$ is always real and nonnegative. If, however, $a \neq b$, the function $F_{ab}(k,\omega)$ can, of course, be complex. Its real part is then known as the cospectrum of fields $\underline{a}$ and $\underline{b}$, and its imaginary part as the quadrature spectrum of these fields. For meteorological applications, it is essential that the above interpretation of the spectrum is also preserved in the more general case of locally isotropic and quasistationary fields, i.e., when only the space-time structure function is independent of x and $\underline{t}$. In this case, the spectrum $F_{ab}(k,\omega)$ can be determined from the structure function by transformations related to the ordinary Fourier transformation (see [4, 5]).

The pure space spectrum $F(k)$ and the pure time spectrum $F(\omega)$ can be defined as in (4), the only difference being that instead of the space-time correlation function $B_{ab}(r,\tau)$, the space function $B_{ab}(r) = B_{ab}(r,0)$ or the time function $B_{ab}(\tau) = B_{ab}(0,\tau)$ must be used here, and the four-dimensional Fourier transform replaced by the three-dimensional or one-dimensional transform. Clearly, the spectrum $F(k)$ can be obtained by integrating the space-time spectrum $F(k,\omega)$ over ω from $-\infty$ to $+\infty$ and the spectrum $F(\omega)$ by integrating $F(k,\omega)$ over the entire space of wave vectors k. Everything said above concerning the spectra of uniform or locally uniform fields also applies for the pure space or pure time spectra.

To determine the space or space-time spectrum, it is necessary to know how the corresponding correlation or structure function depends on r, i.e., to have observational data for a large number of points in space. Such observations are difficult to organize; hence experimental determination of space and space-time spectra is, generally speaking, very complicated. In certain cases, of course, this purpose can be served by data measured aboard an aircraft moving at constant speed V in a fixed direction (for example, in the direction of the Ox axis). Strictly speaking, airborne measurements of field $\underline{a}$ enable us to obtain a population of values of $a(x+r, t+r/V)$ for various $\underline{r}$, i.e., they are useful only for determining certain mixed one-dimensional space-time characteristics. But since the airplane's speed V is usually much greater than both the average wind speed and the typical values of turbulent velocity pulsations, it is often possible to neglect the influence of the time shift r/V if we limit ourselves to not too long distances $\underline{r}$ (or not too small wave numbers $\underline{k}$). In other words, data from aircraft measurements of field $\underline{a}$ can be interpreted in approximation as data on the instantaneous values of $a(x+r, t)$. They can therefore be used for approximate determination of the one-dimensional space structure function $D_{aa}(r)$ and the one-dimensional space spectrum $F^{(1)}_{aa}(k)$ (in the direction of the airplane's flight).

As concerns the pure time spectrum $F_{aa}(\omega)$ (or $F_{ab}(\omega)$), however, its determination requires only values of the field a(x,t) (or the fields a(x,t) and b(x,t)) at a fixed point x, i.e., observational data on the time variation of the meteorological elements at a fixed point in the atmosphere. Such observations are comparatively simple; hence measurements of time spectra are used much more extensively than measurements of space or space-time spectra. In measurement of the time spectrum $F_a(\omega)$, we may start from values of the time correlation function

$$B_{aa}(\tau) = \overline{a(t+\tau)\,a(t)}$$

or the time structure function

$$D_{aa}(\tau) = \overline{[a(t+\tau) - a(t)]^2},$$

where all values of a pertain to the same point x (in practice, probability-theory averaging must, of course, be replaced here by averaging over time). Then, subjecting the empirical functions $B_{aa}(\tau)$ or $D_{aa}(\tau)$ to the Fourier transformation, we can also obtain values of $F_{aa}(\omega)$ from them. It is even more convenient, however, to transform the pulsations a(t) with some sort of transducer into electrical-current pulsations and use a "spectral analyzer" – an analog computer – to make the Fourier transformation. Such an analyzer makes it possible to obtain automatically the values of the Fourier components $a(\Delta\omega)$ of the electrical vibration a(t) corresponding to a series of fixed frequency cells $\Delta\omega$, and then to find the mean squares of these components (or average values of the products of the spectral components $a(\Delta\omega)$ and $b(\Delta\omega)$ of the two oscillations a(t) and b(t)). "Arithmetical filters," which effect the Fourier transformation numerically, may also be used instead of analog devices to isolate the individual spectral components. Such arithmetical filters have also been used widely in recent years; they are particularly easy to build around modern high-speed digital computers.

2. THE TAYLOR "FROZEN TURBULENCE" HYPOTHESIS

The fact that determination of the temporal statistical characteristics of atmospheric turbulence requires only data on the values of the meteorological elements at a single fixed point in the atmosphere greatly simplifies the acquisition of such characteristics. However, time characteristics are inconvenient in that theoretical conclusions usually pertain not to them, but to purely spatial statistical characteristics. Thus, for example, it follows from Kolmogorov's theory of the local structure of turbulence with large Reynolds numbers [2, 6], that all spatial statistical characteristics of the velocity field that depend only on perturbations with rather small scales are independent of average-flow singularities and have a comparatively very simple universal form (see Sections 3 and 4 below). At the same time, it will be a much more complex matter with the time

statistical characteristics, since these characteristics clearly depend on the average wind velocity $\bar{u}$. From the theoretical viewpoint, therefore, it is precisely the purely spatial statistical characteristics that are simplest, and they therefore merit first attention.

The possibility of retrieval of spatial statistical characteristics from the values of the time characteristics, which are much easier to determine experimentally, appears very important in this context. It is well known that as long ago as 1938, G. Taylor [7] advanced the hypothesis that time characteristics can be converted into space characteristics (in the direction of the average flow velocity) by simple replacement of the time shift τ by the space shift $-\bar{u}\tau$, where $\bar{u}$ is the vector of the average velocity. In other words, according to the Taylor hypothesis,

i.e.,
$$B_{ab}(0, \tau) = B_{ab}(-\bar{u}\tau, 0), \quad D_{ab}(0, \tau) = D_{ab}(-\bar{u}\tau, 0), \tag{5}$$

$$\overline{a(\mathbf{x}, t+\tau)\, b(\mathbf{x}, t)} = \overline{a(\mathbf{x}-\bar{u}\tau, t)\, b(\mathbf{x}, t)},$$
$$\overline{[a(\mathbf{x}, t+\tau)-a(\mathbf{x}, t)]\,[b(\mathbf{x}, t+\tau)-b(\mathbf{x}, t)]} = \tag{5'}$$
$$= \overline{[a(\mathbf{x}-\bar{u}\tau, t)-a(\mathbf{x}, t)]\,[b(\mathbf{x}-\bar{u}\tau, t)-b(\mathbf{x}, t)]}.$$

The latter relationships render the sense of Taylor's hypothesis particularly clear: they show that this hypothesis will be valid when turbulent perturbations are transferred by the average flow without changing in the process (when they are, so to speak, "frozen"), so that $a(\mathbf{x}, t+\tau) = a(\mathbf{x}-\bar{u}\tau, t)$. On this basis, the Taylor hypothesis is also commonly known as the "frozen-turbulence hypothesis." In application to spectral characteristics, Equality (5) (if we assume it to be valid for all τ or at least over a large enough range of τ) signifies that

$$F_{ab}(\omega) = \frac{1}{\bar{u}} F_{ab}^{(1)}\left(\frac{\omega}{\bar{u}}\right), \tag{6}$$

where the symbol $F_{ab}^{(1)}(k)$ denotes the one-dimensional spectrum in the direction of the average velocity $\bar{u}$ (which is equal to the one-dimensional Fourier transform of the space correlation or structure function in the direction of vector $\bar{u}$).

The Taylor hypothesis was originally advanced in the context of turbulence behind a grid in a wind tunnel, where the average velocity is constant and approximately two orders larger than the typical turbulent velocity pulsation, and the τ-values of interest do not exceed fractions of a second. Under these conditions, the hypothesis appears perfectly natural. It is therefore not surprising that even Taylor [7] obtained convincing (although indirect) proof of the validity of this hypothesis for turbulence behind the grid, or that subsequent direct comparison of the time and space correlation functions of the velocity field in such turbulence also confirmed it nicely [8]. Applied to atmospheric turbulence, however, where the velocity pulsations

frequently run to several tenths of the average wind speed, and the average wind speed, moreover, varies significantly with altitude, Taylor's hypothesis appears more doubtful. Verification of this hypothesis under atmospheric conditions is therefore of great interest.

One of the first indications of the broad applicability of the Taylor hypothesis to atmospheric turbulence is found in R. Taylor's paper [9], which indicates that the empirical values of the wind field time structure functions in the lowermost layer agree well with the relationships that proceed from Formulas (5) and Kolmogorov's theoretical results on the space structure functions. Later, Panofsky, Cramer, and Rao [10] made a direct comparison of values of the time correlation functions of the longitudinal and transverse wind-speed components u and v at a height of 2 m with the corresponding one-dimensional space correlation functions calculated from the readings of five instruments mounted at the same 2-m height at five points along a fixed straight line (the greatest distance between instruments was 90 m). It was found that in cases when the direction of the average wind speed deviated from the selected straight line by no more than 10°, the measured values of the functions $B_{uu}(\tau)$, $B_{uu}(r)$, $B_{vv}(\tau)$ and $B_{vv}(r)$ satisfied (5) quite well over the entire range of distances r studied. However, the most extensive body of material in confirmation of Taylor's hypothesis for atmospheric turbulence was obtained by comparing data from tower or tethered balloon measurements of turbulence time characteristics with approximate values of the space characteristics found by measuring turbulent pulsations on an airplane flying at high speed at the same height (see page 3). The results of such a check are found, for example, in [11-15]; on the whole, they indicate convincingly that atmospheric turbulence can also be regarded as "frozen" in a broad range of scales for calculation of spectra and correlation functions. By way of example, Fig. 1 presents data obtained at the USSR Academy of Sciences Institute of Atmospheric Physics in simultaneous measurements of the one-dimensional space spectra of the pulsations of the vertical velocity component w and the temperature T on a 70-meter tower (applying hypothesis (6)) and on an airplane flying at 70 m altitude. We see that

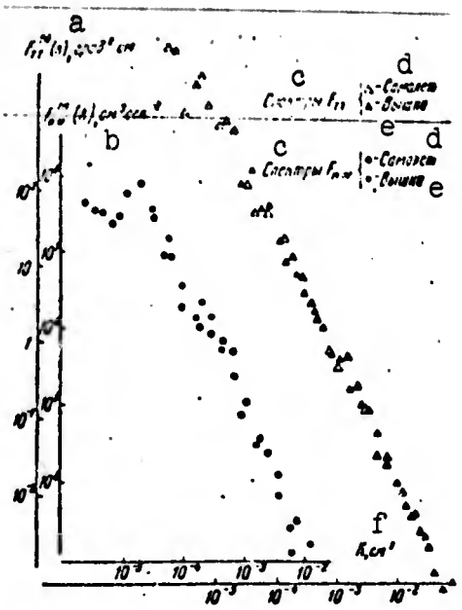

Fig. 1. Spectra of vertical component of wind speed $F^{(1)}_{ww}(k)$ and temperature $F^{(1)}_{TT}(k)$ at height of 70 m, measured simultaneously on airplane and tower. KEY: (a) $deg^2 \cdot cm$ (b) $cm^3 s^{-2}$; (c) spectra; (d) airplane; (e) tower; (f) cm^2.

according to these data, the Taylor hypothesis (6) has a very broad range of applicability (an even broader one than we might have expected).

Needless to say, validity of Equalities (5) and (6) does not yet imply that individual turbulent perturbations in the atmosphere are indeed "frozen in", i.e., that equalities of the type $a(x, t+\tau) = a(x - \bar{u}\tau, t)$ (where a might be understood, for example, as temperature or one of the wind-speed components) necessarily obtain. We note, in addition, that the precise limits of applicability of Taylor's hypothesis to spectra and correlation functions and accurate estimates of its error for turbulent perturbations of various scales have thus far been overlooked.

3. INERTIAL RANGE OF THE TURBULENCE SPECTRUM

Bearing in mind that empirical values of the time spectra of meteorological fields can be transformed by Taylor's hypothesis into values of one-dimensional space spectra in the direction of mean wind, we shall generally consider only space spectra in the material that follows. These spectra are divided into several segments of sharply differing character. We shall begin with that segment which is simplest from the theoretical standpoint, namely, the inertial subrange of the spectrum.

According to the general premises of the Kolmogorov theory, the population of turbulent perturbations with small enough scales (smaller than a certain "external scale" L_0) with sufficiently large Re is always statistically homogeneous and isotropic. The statistical regime of these velocity-field perturbations depends only on two dimensional characteristics – the average dissipation of energy per unit of time in a unit mass of fluid $\bar{\varepsilon}$ (which determines the inflow of energy into the region of small scales from the averaged flow and the large-scale turbulence components) and on the kinetic coefficient of viscosity ν. But the viscosity ν can be substantial only for quite fine perturbations, for which the Reynolds number arrived at from the typical velocity and the typical scale of such a perturbation is of the order of unity (or, more precisely, of the order of the critical value, Re_{cr}). Thus, if we denote the "internal scale" of the turbulence (beginning at which the viscosity becomes significant) by the symbol l_0, then for scales smaller than L_0 but larger than l_0, all static velocity-field characteristics will be determined solely by the variable $\bar{\varepsilon}$. It is this scale interval that is known as the inertial subrange.

In virtue of dimensional considerations, the turbulence spectrum $E(k)$, which is equal to the distribution density of turbulence kinetic energy on the wave-number axis, must, like the one-dimensional spectra (in the mean-wind direction) of the three velocity components $\underline{u}$, $\underline{v}$ and $\underline{w}$ (longitudinal, lateral and vertical), satisfy the universal "5/3 law" of A.M. Obukhov in the inertial subrange of wave numbers $1/L_0 < k < 1/l_0$:

$$E(k) = C\bar{\varepsilon}^{2/3}k^{-5/3}, \qquad F_{uu}^{(1)}(k) = C_1\bar{\varepsilon}^{2/3}k^{-5/3},$$
$$F_{vv}^{(1)}(k) = C_1'\bar{\varepsilon}^{2/3}k^{-5/3}, \qquad F_{ww}^{(1)}(k) = C_1''\bar{\varepsilon}^{2/3}k^{-5/3}. \tag{7}$$

On the basis of isotropy and incompressibility conditions, it is readily deduced that the constant coefficients C, C_1, C_1' and C_1'' are linked by the simple relationships

$$C_1' = C_1'' = \frac{4}{3}C_1, \quad C = \frac{55}{18}C_1. \tag{8}$$

Similarly, the structure functions (3) of components $\underline{u}$, $\underline{v}$ and $\underline{w}$ in the direction of mean wind (i.e., for r parallel to $\bar{u}$) in the inertial subrange $L_0 > r > l_0$ must satisfy A.N. Kolmogorov's "2/3 law":

$$D_{uu}(r) = A_1\bar{\varepsilon}^{2/3}r^{2/3}, \quad D_{vv}(r) = A_1'\bar{\varepsilon}^{2/3}r^{2/3}, \quad D_{ww}(r) = A_1''\bar{\varepsilon}^{2/3}r^{2/3}, \tag{9}$$

where

$$A_1' = A_1'' = \frac{4}{3}A_1,$$
$$A_1 = \frac{3}{2}\Gamma\left(\frac{1}{3}\right)C_1 \approx 4C_1, \quad A_1' \approx 4C_1'. \tag{10}$$

From this we see that both the spectrum and the structure functions of the wind-speed field are uniquely defined in the inertial subrange by the quantity $\bar{\varepsilon}$ and one and only one universal constant, as which any of the coefficients appearing (7) and (9) can be selected.

The first attempt to evaluate the constant A_1 was made as early as 1941 by Kolmogorov [6], who used measured data available at the time on turbulence characteristics behind the grid in a wind tunnel for not very large Re. It is curious that his estimate $A_1 \approx 1.5$ is not too far from what is today regarded as the best value. Later, Obukhov [16] published data from special thermoanemometric measurements of the wind-field structure functions in the atmosphere, which agreed well with the theoretical "2/3 law." Then, estimating $\bar{\varepsilon}$ from the wind profile $\bar{u}(z)$ by the relationship $\bar{\varepsilon} = u_*^3\frac{d\bar{u}}{dz} = \frac{u_*^3}{\varkappa z}$ (where $u_* = \varkappa z\frac{d\bar{u}}{dz}$ is the so-called dynamic velocity or "friction velocity," and $\varkappa \approx 0.4$ is Karman's constant), which are valid for indifferent thermal stratification, Obukhov obtained yet another estimate of the coefficient A_1. Subsequently, numerous empirical data confirming applicability of the theoretical 5/3 and 2/3 laws to atmospheric turbulence were published by a whole series of investigators (see, for example, [9, 16-26]; compare also Figs. 1 and 5). Some of these researchers also attempted to measure the ratio $F_{uu}^{(1)}(k)/F_{ww}^{(1)}(k)$ and compare the results with the theoretical value of $C_1/C_1' = 3/4$. According to MacCready [17, 19], we can only conclude that the ratio $F_{uu}^{(1)}(k)/F_{ww}^{(1)}(k)$ is near unity in order of magnitude; however, the results obtained in [26] from a series of simultaneous

measurements of $F_{uu}^{(1)}(k)$ and $F_{ww}^{(1)}(k)$ on an airplane definitely indicate that this ratio is somewhat smaller than unity in the inertial subrange (equal to 0.61 ± 0.05, which is now not too far from the theoretical 0.75 value). A series of synchronous measurements of the spectra $F_{uu}^{(1)}(k)$ and $F_{ww}^{(1)}(k)$ was carried out at the USSR Academy of Sciences Institute of Atmospheric Physics in 1965 on a 70-meter weather tower near Tsimlyansk; these measurements yielded a value of 0.77 ± 0.08 for the ratio $F_{uu}^{(1)}(k)/F_{ww}^{(1)}(k)$ in the inertial subrange, which is very close to that implied by theory.

However, evaluation of the dimensionless numerical coefficients in the "2/3" and "5/3" laws also requires knowledge of the variable $\bar{\varepsilon}$, and in most cases it has been possible to determine this quantity only from indirect data. It appears that the only exception pertaining to the atmosphere in this respect is the work of Pond, Stewart and Burling [24], in which the spectrum $F_{uu}^{(1)}(k)$ was measured to wave numbers k so large that the exact relation $\bar{\varepsilon} = 15\nu\int_0^\infty k^2 F_{uu}^{(1)}(k)\,dk$ could be used. Hence the value $C_1 \approx 0.47$, which is more reliable than earlier estimates, was obtained in [24]. This result is also in good agreement with the results of other recent measurements of turbulence spectra made in the ocean and in laboratory installations and extending up to very high frequencies (i.e., wave numbers) [27-29]. Finally, we note that there is one more method of independent determination of the coefficient C_1 (or $A_1 \approx 4C_1$) based on the exact relation derived by Kolmogorov [6]:

$$A_1 = \left(-\frac{5}{4}S\right)^{-2/3} \approx 0{,}86\,(-S)^{-2/3},$$
$$S = \frac{\overline{[u(x+\bar{u}r) - u(x)]^3}}{\{\overline{[u(x+\bar{u}r) - u(x)]^2}\}^{3/2}} = \text{const.} \qquad (11)$$

Gurvich [30] measured S in the lowermost layer of the atmosphere; the results yielded a value of A_1 that was slightly smaller than the earlier evaluations in [24, 27], but much of the disagreement can be eliminated by introducing corrections into Gurvich's data to take instrumental averaging into account [31]. As a result, we may conclude that the data of recent years finally make it possible to determine C_1 (and, consequently, the values of all other constants in (7) and (9)) accurate to within 10-15%; at the present time, the best estimate of C_1 is $C_1 \approx 0.45$-0.50.

If we assume that the constants in the "5/3 laws" (i.e., in Formulas (7)) are known, we need only know the average energy dissipation $\bar{\varepsilon}$ to determine the velocity spectrum in the inertial subrange. Thus, study of the inertial subrange of the spectrum reduces to study of the distribution of a single characteristic $\bar{\varepsilon}$ in the atmosphere. Many different methods exist for determination of this quantity: starting from the equation of turbulent energy balance from the mean profiles $\bar{u}(z)$ and $\bar{T}(z)$ and the

turbulent flows of momentum $\tau = \rho u_*^2$ and heat q or even from the profiles $\overline{u}(z)$ and $\overline{T}(z)$ alone [16, 22, 32, 33]; from observational data on the turbulent diffusion of impurities [34, 35]; from empirical values of the structure function, some integral of the structure function or the spectrum [17, 19, 23, 25, 33, 37, 39, 40], and certain others. Several summary diagrams of $\overline{\varepsilon}$ as a function of height z have also been published from the data of various authors [36-38]. In many cases, however, the results obtained thus far are based on numerical coefficients of inadequate reliability, often show very low accuracy and wide scatter of the values found for $\overline{\varepsilon}$, and, in many cases, even contradict one another; they are also still quite incomplete.

In the lowermost atmospheric layer, the values of $\overline{\varepsilon}$, reduced to dimensionless form by dividing by the combination $u_*^3/\kappa z$, should be a universal function $e(\zeta)$ of the variable $\zeta = z/L$, where $L = -\frac{c_p \rho T_0 u_*^3}{\kappa g q}$ is the scale that figures in the familiar Monin-Obukhov similarity theory [41]; however, little study has as yet been given to the form of the function $e(\zeta)$ [33]. The frequently encountered determinations of the function $e(\zeta)$ by means of the equation of turbulent-energy balance are not rigorous in that certain terms that may not be negligibly small are invariably dropped. For indifferent stratification, the balance equation reverts to the equality $\overline{\varepsilon} = u_*^3/\kappa z$, and for very strong instability in free-convection conditions to the equality $\overline{\varepsilon} = \frac{g}{T_0}\frac{q}{c_p \rho}$. These results no longer require special assumptions for their derivation and contain no unknown numerical coefficients; however, they have not, to the best of our knowledge, been verified empirically by independent determination of $\overline{\varepsilon}$ by other methods. In the free atmosphere, the situation is more complex, but in principle $\overline{\varepsilon}$ should be uniquely defined even here by height above ground level and general meteorological conditions (as well as by the type of underlying surface). The importance of considering thermal-stratification conditions was convincingly demonstrated by Ivanov [37, 39] with reference to data pertaining to the 300-meter bottom layer of the atmosphere (above terrain characterized by complex relief and a nonuniform cover of vegetation). In the papers of Zubkovskiy [23] and Koprov [25], values of $\overline{\varepsilon}$ under typical summer conditions of developed convection over a steppe were determined by measuring the spectral density $F_{ww}^{(1)}(k)$ on an airplane for a single value of k in the inertial subrange; it was found that $\overline{\varepsilon}$ varies comparatively slightly under these conditions in the layer from 50 to approximately 1000 m, and then begins to diminish rapidly with increasing altitude. An attempt may be made to compare the relative constancy of $\overline{\varepsilon}$ in this thick layer with the theoretical conclusion that $\overline{\varepsilon} = \frac{g}{T_0}\frac{q}{c_p \rho} = \text{const}$ under conditions of free convection, but this comparison is not very viable, since the turbulent heat flow

q varies markedly between $z = 50$ m and $z = 1000$ m (see Section 5) and the observed values of ε for 50 m < z < 1000 m are found to be considerably smaller than the synchronous values of ε in the free-convection layer near the ground. Recently, the method of determining ε that was used in [23, 25] was applied by Koprov and Tsvang [42] to determine ε as a function of height z above the steppe for various thermal-stratification conditions. It was found that the $\bar{\varepsilon}(z)$ profiles for the middle of a clear summer day (i.e., under developed-convection conditions), early in the morning (under conditions of developing convection, when the stratification near the ground is already unstable, and a temperature inversion is observed at greater heights) and in the evening (when, except for the few lowermost tens of meters, stratification is nearly indifferent) differ sharply from one another, but are almost always of the same nature on different days with similar weather conditions. Figure 2 shows mean profiles of $\bar{\varepsilon}(z)$ for the three meteorological situations indicated.

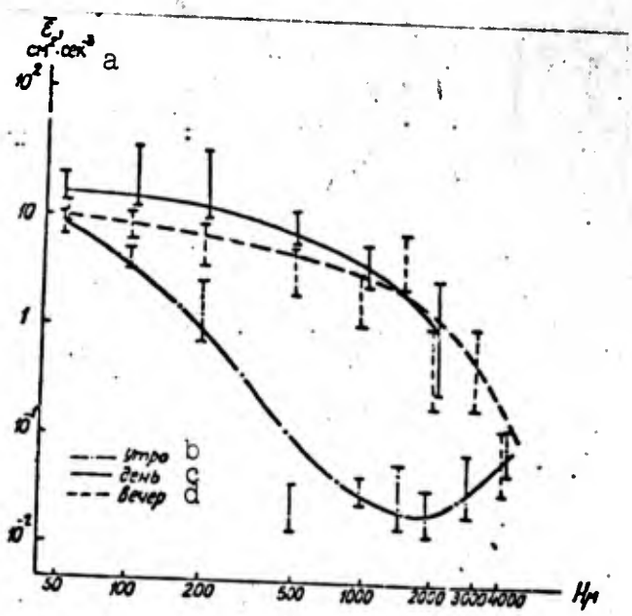

Fig. 2. Mean profiles of $\bar{\varepsilon}$ at various times of day. The vertical ticks represent twice the standard deviations at the various altitudes.
KEY: (a) $cm^2 \cdot s^{-3}$; (b) morning; (c) afternoon; (d) evening.

The inertial-subrange concept is also applicable to temperature-field perturbations (although it would be more correct in this case to speak not of an inertial, but of a convective subrange, we elect not to introduce a new term here). Here the "inertial subrange" should be understood as an interval of scales in which the statistical regime is homogeneous and isotropic and depends neither on the specific peculiarities of the mean fields u and $\overline{T}$ nor on the molecular coefficients of viscosity and thermal conductivity. Since the Prandtl number of air is near unity,

and the distances over which wind speed and temperature change substantially do not differ greatly from one another in the atmosphere, the inertial subrange for the temperature field will be bounded by the scales L_1 and l_1, which are of the same orders as L_0 and l_0, respectively. In this subrange, all statistical velocity-field characteristics will be determined by the quantity $\bar{\varepsilon}$ and the related $\bar{\varepsilon}_T = \chi \sum_i \overline{\left(\frac{\partial T}{\partial x_i}\right)^2}$ (where χ is the molecular coefficient of thermal diffusivity), which is known as the "temperature-nonuniformity equalization rate" or the "temperature dissipation." Here, by virtue of dimensional considerations, we obtain a "5/3 law" for the temperature spectrum $E_T(k)$ and the one-dimensional temperature spectrum $F_{TT}^{(1)}(k)$ in the inertial subrange $1/L_1 < k < 1/l_1$:

$$E_T(k) = C_T \bar{\varepsilon}_T \bar{\varepsilon}^{-1/3} k^{-5/3}, \quad F_{TT}^{(1)}(k) = C_T' \bar{\varepsilon}_T \bar{\varepsilon}^{-1/3} k^{-5/3}, \tag{12}$$

and a "2/3 law" for the structure function of temperature $D_{TT}(r)$ $L_1 > r > l$ [43, 44]:

$$D_{TT}(r) = A_T \bar{\varepsilon}_T \bar{\varepsilon}^{-1/3} r^{2/3}. \tag{13}$$

The coefficients C_T, C_T' and A_T are connected by the relationships

$$C_T' = \frac{3}{5} C_T, \quad A_T = \frac{3}{2} \Gamma\left(\frac{1}{3}\right) C_T' \approx 4 C_T', \tag{14}$$

since it is sufficient to know one of them to determine all the rest.

The earliest empirical data in confirmation of the "2/3 law" (13) were obtained by Krechmer [45], Shiotani [46], and Tatarskiy [47]. Later, several authors also obtained experimental confirmation of the "5/3 law" (12) for the temperature spectrum (see, for example, [48-51, 29] and Fig. 1). To determine numerical values of the coefficients in these laws, however, it is necessary to know the quantities $\bar{\varepsilon}$ and $\bar{\varepsilon}_T$, of which the latter is difficult to determine with sufficient reliability. The simplest way to find $\bar{\varepsilon}_T$ is to use the balance equation of temperature pulsation intensity $\overline{T'^2}$ (where $T' = T - \bar{T}$) and empirical data on the profiles $\bar{u}(z)$ and $\bar{T}(z)$ and the turbulent flows τ and q (see, for example, [47, 52]). In the balance equation, however, it is necessary to disregard the term describing the vertical diffision of $\overline{T'^2}$; moreover, the results obtained may also be distorted by the nonuniformity of the underlying surface and errors in measuring τ and q. The first attempt to use this method, which was made by Tatarskiy [47], who has only data on mean profiles $\bar{u}(z)$ and $\bar{T}(z)$, resulted in the rough estimate $A_T \approx 6$. Later, Gurvich and Zubkovskiy [52] processed Tsvang's numerous measurements by a similar method and obtained $A_T \approx 2.7$, while Takeuchi [33] showed that the data from earlier similar measurements made in Australia by Swinebank and

R. Taylor result in a much lower estimate, $A_T \approx 1.2$. It must be remembered, however, that both Tatarskiy's data and those used by Takeuchi are rougher than those of [48], and that Tatarskiy's and Takeuchi's estimates were obtained with practically no consideration of the effect of thermal stratification, which reduces their accuracy substantially; hence neither of the estimates $A_T \approx 6$ and $A_T \approx 1.2$ (which disagree very sharply) inspires much confidence. On the other hand, the A_T value obtained by Gibson and Schwartz [29] from measurements of turbulence characteristics behind a grid in a wind tunnel, where $\bar{\varepsilon}$ and $\bar{\varepsilon}_T$ can be determined quite reliably from the curve of decay of the mean-square velocity and temperature with increasing distance from the grid, was found to agree elegantly with the estimate of [52]: according to Gibson and Schwartz (with consideration of the fact that these authors use the term "temperature dissipation" for a quantity twice as large as $\bar{\varepsilon}_T$) $C_T \approx 0{,}7$, i.e., $A_T \approx 2{,}8$. Also in satisfactory agreement with this last estimate is the result obtained in [52] by application of the exact equality due to Yaglom [53]

$$A_T = -\frac{4}{3F}\left(-\frac{5S}{4}\right)^{1/3},$$

$$F = \frac{\overline{[u(\mathbf{x}+\bar{\mathbf{u}}r)-u(\mathbf{x})][T(\mathbf{x}+\bar{\mathbf{u}}r)-T(\mathbf{x})]^2}}{\{\overline{[u(\mathbf{x}+\bar{\mathbf{u}}r)-u(\mathbf{x})]^2}\}^{1/2}\overline{[T(\mathbf{x}+\bar{\mathbf{u}}r)-T(\mathbf{x})]^2}} = \text{const}, \qquad (15)$$

where S has the same content as in (11). That is to say, according to [52], calculation of A_T by this formula (in which S and F were determined from a comparatively short time trace of wind-speed and temperature pulsations at two not widely separated points in the ground layer of the atmosphere), yielded $A_T \approx 3.5$. Thus, the presently available estimates of the numerical coefficients in the "two-thirds" and "five-thirds" laws for the temperature field, even though they are still widely scattered, nevertheless give the impression that the coefficient A_T is somewhere around 3 ($A_T \approx 2.8$ can be recommended as most defensible), while the coefficient C_T' is close to 0.7.

If the values of the numerical coefficients (12) and (13) were known, data on the spectra $F_{TT}^{(1)}(k)$ and $F_{uu}^{(1)}(k)$ for the same k within the inertial subrange would enable us to determine the characteristics $\bar{\varepsilon}$ and $\bar{\varepsilon}_T$ simultaneously. At the present time, however, it is more convenient to restrict ourselves to data on the energy dissipation $\bar{\varepsilon}$ and the combination $\varepsilon_T \bar{\varepsilon}^{-1/3}$ or, even better, on the combination $B_T = A_T \bar{\varepsilon}_T \bar{\varepsilon}^{-1/3}$, which is simplest to determine from values of $F_{TT}^{(1)}(k)$. It follows from Tsvang's measurements [49] that under typical summertime conditions of developed convection over the steppe, B_T decreases with altitude approximately in proportion to $z^{-4/3}$ beginning at z = 50 m and continuing up to the height at which the potential-temperature gradient changes sign; at higher altitudes, however, we usually observe a substantially faster decrease of B_T with altitude. Under nighttime inversion conditions, B_T decreases with altitude more rapidly

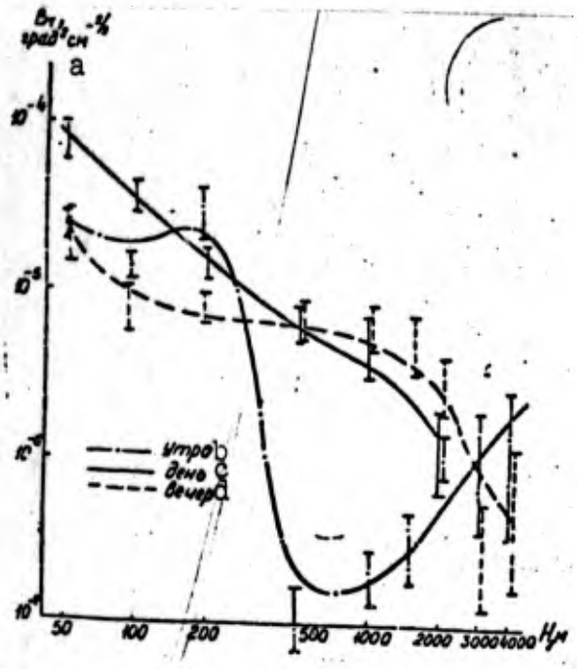

Fig. 3. Mean profiles of $\overline{B_T}$ for various times of day. Symbols same as in Fig. 2.
KEY: (a) $deg^2 cm^{-2/3}$; (b) morning; (c) afternoon; (d) evening.

Fig. 4. B_T as a function of potential-temperature gradient $\frac{\partial \overline{\vartheta}}{\partial z} + \gamma_a = \gamma_a - \gamma$ under conditions of stable stratification. γ_a = 1°/100m is the dry adiabatic temperature gradient.

than during the day. Results pertaining to developed-convection conditions are also confirmed by the data of subsequent measurements by Koprov and Tsvang [42], where it is found that the relation $B_T = B_0 z^{-4/3}$, where B_0 = const, is satisfied quite well beginning at a height of the order of a few meters (this z-curve of B_T can also be justified theoretically in the ground layer for free convection; cf. [54]). At the same time, during the early morning hours, when a powerful temperature inversion begins at altitudes of the order of 50-250 m, B_T remains approximately constant up to the lower boundary of the inversion, then increases slightly and, finally, drops sharply (by 2-3 orders); at higher altitudes, we observe a new (but not very fast) increase of B_T during this time. In later afternoon hours, when the temperature gradient becomes nearly adiabatic up to altitudes of the order of 1500 m, B_T remains approximately constant up to this height, above which it begins to decrease. Figure 3 shows the general appearance of the corresponding B_T profiles. It is curious that in all three of the meteorological situations considered, the B_T-profiles are found to be very closely related to the mean temperature profiles (see, for example, Fig. 4, which shows B_T as a function of the potential-temperature gradient $\frac{\partial \overline{\vartheta}}{\partial z} = \gamma_a - \gamma$ for the morning hours, as obtained from averaged

profiles of these quantities).

Results pertaining to the inertial subrange of the temperature-pulsation spectrum are also applicable to the pulsation spectra of humidity, electron density in the ionosphere, or the concentration of any other passive impurity. In this case, the "temperature dissipation" $\bar{\varepsilon}_T$ must be replaced by the appropriate characteristic of the concentration field under consideration; however, the old values of the coefficients C_T, C_T' and A_T must be retained (if we accept the idea that temperature can also be regarded as a passive impurity in the inertial subrange). Data on the pulsation spectrum of salt concentration in water, obtained under laboratory conditions and in good agreement with the "5/3 law" can be found in [29]. Data confirming the "5/3 law" for humidity pulsations in the atmosphere can be obtained most simply by refractometric measurements, since humidity has considerable influence on the refractive index for radio waves; other papers of the present colloquium discuss this in greater detail.

4. INFLUENCE OF MOLECULAR VISCOSITY AND THERMAL CONDUCTIVITY ON THE SPECTRA OF THE METEOROLOGICAL FIELDS

The inertial range is bordered on its small-scale (i.e., large-wave-number) end by the so-called viscous subregion – the population of the smallest-scale velocity-field perturbations, which are now influenced directly by molecular viscosity. In this subrange, all velocity-field statistical characteristics are determined by the two dimensional variables $\bar{\varepsilon}$ and ν. For example, the scale or wave number defining the boundary of the viscous subregion must also be determined by these variables. Hence it follows that viscosity begins to influence static turbulence characteristics strongly beginning at the scale $l_0 = a_0\eta$ or wave number $k_0 = a_1/\eta$, where a_0 and a_1 are universal constants and $\eta = \nu^{3/4}\bar{\varepsilon}^{-1/4}$ is the so-called Kolmogorov microscale.

The values of the coefficients a_0 and a_1 are not, of course, determined fully accurately – they depend on determination of the viscous-subregion boundary l_0 or k_0, which may be arbitrary to a significant degree. It is natural to assume that $a_0 = (a_1)^{-1}$, although if we require that the "2/3 law" for $r = l_0$ and the "5/3 law" for $k = k_0$ have the same accuracy, $(a_1)^{-1}$ may also be found not to agree with a_0. MacCready [19] proposed a rigorous definition of the scale l_0 with which he found that $a_0 \approx 15$, $a_1 \approx 1/15$; he showed simultaneously that it is even more convenient in certain respects to assume that $a_0 \approx 1$. At the present time, however, it is expedient to evaluate the coefficients a_0 and $a_1 = 1/a_0$ on the basis of the highly accurate empirical values of the spectrum $F_{uu}^{(1)}(k)$ given in [24, 27] for a broad range of k-values (which even cover part of the viscous subrange). According to these data, the spectrum $F_{uu}^{(1)}(k)$ begins to deviate markedly from the "five-thirds law" beginning approximately at $k_0 \approx 1/8\eta$; also near this k_0 value is the maximum of the one-dimensional energy-dissipation spectrum (which is proportional to $k^2 F_{uu}^{(1)}(k)$). For these two reasons, the estimates

$k_0 = 1/8\eta$ and $\ell_0 = 8\eta$ can be regarded as a reasonable estimate of the boundary between the viscous subrange and the inertial interval. In the atmosphere's ground layer (at a height of one or a few meters above the ground), the values of $\bar{\varepsilon}$ are usually of the order of 10^2-10^3 cm^2/s^3 (these data pertain to daytime summer conditions in the region of the South Russian steppe); hence η is usually included here between 0.04 cm and 0.07 cm, and ℓ_0 between 0.3 cm and 0.6 cm. According to Fig. 2, ℓ_0 is of the order of 1 cm at a height of 50 m, and at 1000 m it is usually between 1 cm and 5 cm; with a further increase in altitude, ℓ_0 continues to increase, and, for example, at an altitude of the order of 100 km it is reckoned in tens of meters.

In the viscous subregion, the spectra and structure functions are given by formulas of the type

$$E(k) = \bar{\varepsilon}^{1/4} k^{-1/4} \varphi_1(k\eta), \qquad F_{uu}^{(1)}(k) = \bar{\varepsilon}^{1/4} k^{-1/4} \varphi_2(k\eta),$$
$$F_{vv}^{(1)}(k) = F_{ww}^{(1)}(k) = \bar{\varepsilon}^{1/4} k^{-1/4} \varphi_3(k\eta) \tag{16}$$

and

$$D_{uu}(r) = \bar{\varepsilon}^{1/2} r^{1/2} \psi_1(r/\eta), \quad D_{vv}(r) = D_{ww}(r) = \bar{\varepsilon}^{1/2} r^{1/2} \psi_2(r/\eta), \tag{17}$$

where all one-dimensional spectra and structure functions are taken in the direction of the mean wind and ϕ_1, ϕ_2, ϕ_3, ψ_1, and ψ_2 are universal functions of a single variable that are uniquely related to one another by simple relationships. The "5/3" and "2/3" laws are expressed in this notation by the asymptotic relationships $\varphi_1(x) \to C = \text{const}$, $\varphi_2(x) \to C_1 = \text{const}$, $\varphi_3(x) \to C_1 = \text{const}$ as $x \to 0$ and $\psi_1(y) \to A_1 = \text{const}$, $\psi_2(y) \to A_1 = \text{const}$ as $y \to \infty$. For $y = r/\eta \ll 1$, the functions $\psi_1(y)$ and $\psi_2(y)$ satisfy the very simple asymptotic relationships $\psi_1(y) \approx y^{4/3}/15$ and $\psi_2(y) \approx 2y^{4/3}/15$, which were long ago stated by Kolmogorov [6]. Until comparatively recently, it was generally supposed that for x comparable with unity, values of the functions $\phi_1(x)$, $\phi_2(x)$ and $\phi_3(x)$ could be given by one or another semiempirical formula, of which a whole series were proposed at various times by Obukhov, Heisenberg, Kovazhnyy and other authors (see, for example, Chapter 6 in the book [3]). However, there is no justification at all for this approach, since the theoretical considerations on which all of the proposed semiempirical formulas are based (including even the most recent, [55]) are in fact inapplicable to the viscous subrange. Developing certain ideas of Townsend and Batchelor, Novikov [56] recently advanced a physically better-grounded argument on the behavior of the turbulent spectrum in the range of the largest wave numbers $k \gg 1/\eta$, i.e., on the asymptotic behavior of the functions $\phi_1(x)$, $\phi_2(x)$ and $\phi_3(x)$ as $x \to \infty$ (cf. also Saffman [57]); however, these considerations pertain to a spectral range on which there are as yet no experimental data. At the present time, therefore, we can advance only certain grossly preliminary hypotheses on the possible form of the functions ϕ_1, ϕ_2, and ϕ_3, basing them on the experimental data of [24, 27-29], in which the initial segment of a universal curve describing the spectrum $F_{uu}^{(1)}(k)$ in the viscous subregion was studied. For example, Gorshkov [58] proposed for the function $\phi_2(x)$ an empirical formula of

the type

$$\varphi_2(x) \approx 0{,}48 \exp\left\{-\frac{40x^2}{1+40x^2} - 5x^2\right\} \qquad (18)$$

and obtained fairly good agreement with available empirical data (Fig. 5). We note that Formula (18) also agrees qualitatively with Novikov's reflections on the asymptotic behavior of the spectrum as $k\eta \to \infty$.

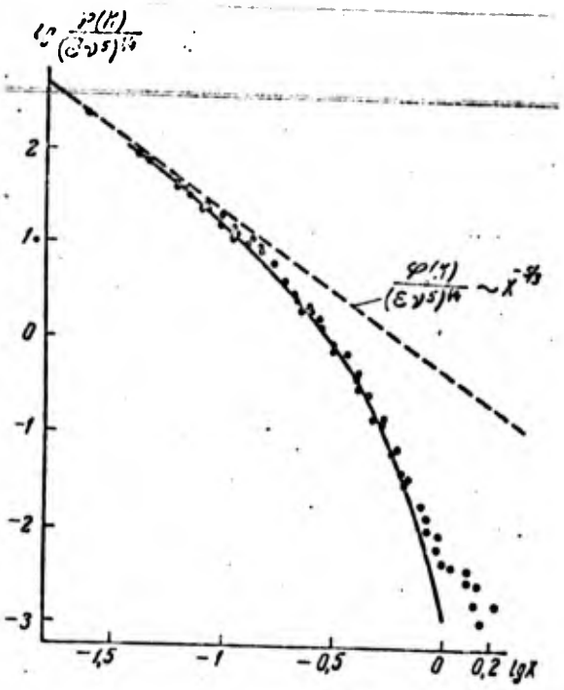

Fig. 5. Comparison of N.F. Gorshkov's empirical formula for the function $\phi_2(x)$ with measured results on the spectrum $F_{uu}^{(1)}(k) = \varphi(k)$.

The situation is even more backward as regards the behavior of the temperature-field statistical characteristics (or passive-impurity concentration) in the range of very small scales or very large wave numbers. These statistical characteristics now depend on the four dimensional variables $\bar{\varepsilon}$, $\bar{\varepsilon}_T$, ν, and χ, where χ is the molecular coefficient of thermal diffusivity or diffusion; hence we obtain relationships of the following form for the structure function and spectrum:

$$D_{TT}(r) = \bar{\varepsilon}_T\, \bar{\varepsilon}^{-1/3} r^{1/3} \psi_T(r/\eta, \mathrm{Pr}),$$
$$\mathrm{Pr} = \nu/\chi \qquad (19)$$

and

$$E_T(k) = \bar{\varepsilon}_T \bar{\varepsilon}^{-1/3} k^{-5/3} \varphi_T(k\eta, \mathrm{Pr}),$$
$$F_{TT}^{(1)}(k) = \bar{\varepsilon}_T \bar{\varepsilon}^{-1/3} k^{-5/3} \varphi_T^{(1)}(k\eta, \mathrm{Pr}), \qquad (20)$$

which contain universal functions of two variables. In virtue of the "2/3" and "5/3" laws, $\psi_T(y, \mathrm{Pr}) \to A_T$ as $y \to \infty$, $\varphi_T(x, \mathrm{Pr}) \to C_T$ and $\varphi_T^{(1)}(x, \mathrm{Pr}) \to C_T'$ as $x \to 0$. The values $r = \ell_1$ and $k = k_1$ beginning at which these laws can be applied must obviously be of the form $\ell_1 = a_T\eta$ and $k = a_T'/\eta$, where a_T and $a_T' \sim (a_T)^{-1}$ are functions of the Prandtl number, for which there is as yet almost no information. It is easily shown that $\psi_T(y, \mathrm{Pr}) \approx \mathrm{Pr} \cdot y^{4/3}/3$ for $y \ll 1$ (see [43, 53]); as concerns the theoretical derivations pertaining to the functions $\phi_T(x,\mathrm{Pr})$ and $\phi_T^{(1)}(x,\mathrm{Pr})$ however, they are limited to only a few general considerations on the asymptotic behavior of these functions as $x \to \infty$ (see [59-61, 57]). Empirical data on the values of $\varphi_T^{(1)}(x, \mathrm{Pr})$ are much more spotty than even the available data on the function $\phi_2(x)$ of one variable; they appear to be exhausted by the results of Gibson and Schwartz [29] and the as yet unpublished and highly preliminary conclusions obtained by Grant and Stewart in measurements of the temperature-pulsation

spectrum in the ocean. We note incidentally that both the data of Gibson and Schwartz and those of Grant and Stewart pertain to measurements in water at relatively large Prandtl numbers; hence they bear no relation at all to atmospheric-turbulence spectra.

5. CHARACTERISTICS OF NONISOTROPIC TURBULENT PERTURBATIONS. CERTAIN SINGLE-POINT MOMENTS

Bordering the inertial subrange at its large-scale (i.e., small-wave-number) end is the enormous region of nonisotropic turbulent perturbations, whose horizontal dimensions in the atmosphere may vary from a few tens or hundreds of meters to thousands of kilometers. In conclusion, we shall dwell briefly on certain problems with a bearing on such nonisotropic perturbations and the closely related single-point moments of the meteorological fields.

Disturbance of isotropy has a whole series of important consequences that admit of experimental verification. Here the turbulence spectra (both $E(k)$ and $E_T(k)$ and the one-dimensional spectra) cease to satisfy the universal "5/3 laws," and the structure functions the "2/3 laws"; the one-dimensional spectrum of the longitudinal velocity component begins to deviate from the spectrum of the vertical or lateral component multiplied by 3/4; the vertical-velocity pulsations begin to correlate with the pulsations of horizontal velocity and temperature, with the result that turbulent heat flows and momenta make their appearance, and so forth. Each of these consequences may be taken as a characteristic criterion of perturbation anisotropy; hence the boundary of the inertial subrange on the large-scale end can be determined by many different methods, which often lead to widely differing results. From the theoretical standpoint, it appears most natural to take as the boundary of the inertial subrange the scale L_0 corresponding to the wave number $\underline{k}$ beginning at which the spectral tensor of the velocity field becomes essentially anisotropic, while the function $E(k)$ deviates significantly from $C\varepsilon^{2/3}k^{-5/3}$. Otherwise, we might also consider the scale L_1 or wave number k_1 beginning at which the temperature spectrum $E_T(k)$ deviates substantially from the "5/3 law"; the scales L_0 and L_1 will apparently be quite close to one another in many cases, although they do not agree exactly. Unfortunately, it is very hard to determine the two scales L_0 and L_1, since it is almost impossible to measure the three-dimensional spectrum reliably. In practice, therefore, it is much more convenient to deal with scales that can be defined from the one-dimensional spectrum. It is essential that the one-dimensional spectra usually begin to deviate markedly from the "5/3 law" at considerably smaller wave numbers (i.e., larger scales) than the corresponding three-dimensional spectrum $E(k)$ or $E_T(k)$. This is because the values of $F_{uu}^{(1)}(k)$ and $F_{ww}^{(1)}(k)$ (or $F_{TT}^{(1)}(k)$) are obtained from $E(k')$ (or $E_T(k')$) by integrating over $\underline{k}$ from $k' = k$ to $k' = \infty$; hence the inertial subrange of the spectrum $E(k')$ or $E_T(k')$ also makes the basic contribution to the values of the one-dimensional spectra $F_{uu}^{(1)}(k)$, $F_{ww}^{(1)}(k)$ or $F_{TT}^{(1)}(k)$ over a substantial range of wave numbers

k smaller than k_0 or k_1 (see Gifford's paper [62], which examines this effect in context with the one-dimensional spectrum $F_{uu}^{(1)}(k)$, for which it is particularly strongly in evidence). Also apparently related to this circumstance is the fact that the measured spectra of turbulent momentum and heat flows are often found to be intrinsically nonzero at k for which the one-dimensional velocity and temperature pulsation spectra still satisfy the five-thirds law quite exactly, although these flows must obviously be zero for isotropic turbulent pulsations. A brief survey of the problem of the various definitions of the inertial subrange boundary may be found in MacCready's paper [19] along with tentative estimates of the differences between these boundaries.

Physically, deviations from isotropy may be caused by many widely diverse factors – for example, the influence of the underlying surface, in which vertical scales exceeding the distance z to the ground are cut off; or by the presence of a vertical wind-speed gradient characterized by the scale $\bar{u}\left|\frac{d\bar{u}}{dz}\right|^{-1}$; or by the action of Archimedean forces (which appear essentially beginning at the so-called "Bolgiano-Obukhov scale" $L_* = \bar{\varepsilon}^{1/4}\bar{\varepsilon}_T^{-3/4}(g/T)^{-1/4}$, for which see [63, 64]); or by the influence of nonequilibrium temperature stratification (characterized locally by the "Vaysal frequency" $\omega_0 = \left\{\frac{g}{T_0}\left|\frac{\partial\bar{T}}{\partial z} + \gamma_a\right|\right\}^{1/2}$, where γ_a is the adiabatic temperature gradient). As a result, in the lowermost 100-200 m, the scale beginning at which the turbulence anisotropy begins to manifest can apparently be regarded as proportional to the altitude z, with the proportionality factor depending on temperature stratification; higher, however, it is most probably determined primarily by stratification. Curiously, when this scale is determined from the value of the wave number at which the one-dimensional horizontal spectra begin to deviate markedly from the "five-thirds law," or on the basis of the r at which the horizontal structure functions begin to deviate markedly from the "two-thirds law," it is usually found that the boundary of the isotropic range considerably exceeds the distance to the ground. On the whole, however, the question of the boundary of the atmospheric-turbulence inertial range at the large-scale end has been studied quite inadequately up to the present time; certain grossly preliminary data on this subject can be found in [19] (see also [25]).

Beyond the boundary of the inertial range, the turbulence spectrum begins to increase with decreasing wave number more slowly than $k^{-5/3}$; thereafter, however, it usually even begins to decrease (passing through its maximum at a certain k_2). The scale corresponding to k_2 is also an important turbulence characteristic: it determines the characteristic dimensions of the perturbations containing most of the turbulent energy. In determining this scale, it is again necessary to limit ourselves to quantities related to the one-dimensional spectra; most convenient and most frequently used are scales determined from the

maximum of the function $kF^{(1)}(k)$. Consideration of precisely this combination $kF^{(1)}(k)$ results from the fact that in practice it is more convenient over a very broad range of scales to represent the spectrum graphically, with the wave numbers plotted against a logarithmic axis; the function $kF^1(k)$ will then be equal to the distribution density on the log k axis. Thus we see that the maximum of the density curve is in fact not a very accurate characteristic, since it depends on the selection of the scale for the axis of abscissas; in this case, this works in our favor, since on conversion to the logarithmic wavenumber scale, the spectral-density maximum shifts into a region of larger k (i.e., shorter distances), so that it is easier to detect on empirical data. Nevertheless, even the scale corresponding to the maximum of $kF^{(1)}(k)$ is usually found to be very large under the conditions of the open atmosphere; hence its determination requires use of large-scale averaging and is possible only with apparatus that can register low-frequency oscillations without distortion.

Three different scales L_u, L_w and L_T will, of course, correspond to the maxima of the functions $kF_{uu}^{(1)}(k)$, $kF_{ww}^{(1)}(k)$ and $kF_{TT}^{(1)}(k)$ Empirical data on the values of all these scales for various heights and various stratifications are still very spotty; some preliminary results in this regard can be found in Lumley and Panofsky's book [65] and in [25, 66, 67]. Results from measurements of one-dimensional spectra made at the USSR Academy of Sciences Institute of Atmospheric Physics indicate that the scale L_w is usually conspicuously smaller than both L_u and L_T; however, reliable determination of quantitative relationships among these three scales requires much more work.

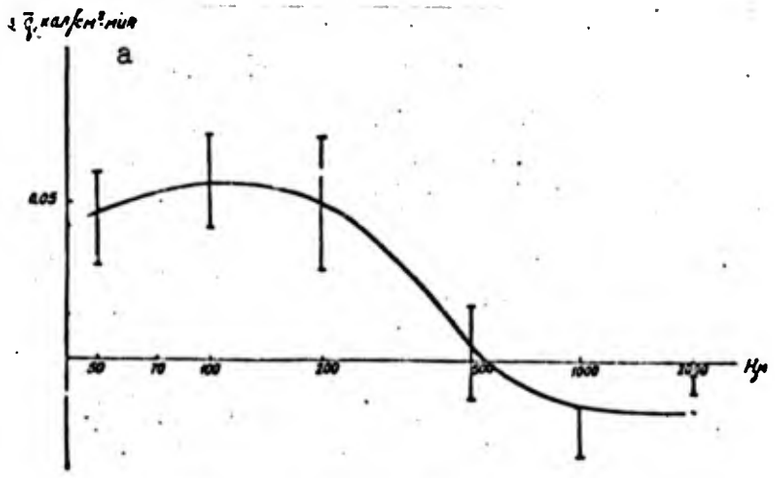

Fig. 6. Mean profile of turbulent heat flow q(z) in the daytime over the steppe. KEY: (a) cal/cm²·min.

The range of nonisotropic turbulent perturbations makes the basic contribution to the values of all single-point moments of

the meteorological fields. Among these single-point moments, the root-mean-square values σ_u, σ_v, σ_w, and σ_T of the pulsations u', v', w', and T' of the three velocity components and the temperature usually attract more than proportional attention. A summary of available data on these quantities can be found, for example, in Lumley and Panofsky's book [65] (see also the later papers [68], and [69]); it must be remembered, however, that data obtained on them by various investigators quite frequently disagree. It should be noted in this connection that it is not easy to define exactly what should be meant under the conditions of the atmosphere by the dispersions σ_u^2, σ_w^2, etc. The point is that the spectra of atmospheric pulsations are not cut off sharply at any frequency, but merge smoothly into the mesoturbulent and then the macroturbulent ranges (from which the micropulsation spectrum is at best separated only by a comparatively broad valley; cf. Lumley and Panofsky [65], Kolesnikova and Monin [70], Byzova, Ivanov and Morozov [69]). Hence all available data on the dispersions of turbulent pulsations are to some extent arbitrary and based on an artificial cutoff of the spectrum at a certain definite frequency that is different for different investigators. On this basis, it might occur to us that before attempting to systematize data on σ_u, σ_w, etc., an attempt should be made to study as thoroughly as possible the spectra of these pulsations in the low-frequency range in order to refine our information on the position and nature of the "valley" in the spectrum, which is necessary to understand exactly what sense the corresponding dispersions may have.

Among the mixed single-point moments, the most important are, of course, the moments $-\tau/\rho = \overline{u'w'}$ and $q/c_p\rho = \overline{T'w'}$, which define turbulent transfer of momentum and heat. These quantities also have a broad spectrum extending all the way to relatively low frequencies; this is why reliable measurements require thorough investigation of the cross spectra of the pulsations u' and w' or T' and w'. Preliminary measurements of the heat-flow and momentum spectra (i.e., the cospectra of the pulsations T' and w' or u' and w') carried out by Gurvich and Tsvang (see [71]) create the impression that these spectra are also approximately proportional to f^{-1} over a comparatively broad range in both the ground layer and in the free atmosphere. However, this fact cannot yet be explained theoretically and is not very certain. The quantities q and τ themselves have been measured many times in the ground layer by a whole list of investigators (see, for example, §8 of the book [1], which contains an extensive bibliography on the problem). No direct measurements of τ have, to our knowledge, been made in the free atmosphere, while measurements of the turbulent heat flow q are just being started now and have thus far been of relatively modest accuracy (see [15, 72, 73]). The data of Kaprov and Tsvang [15], which also agree generally with those of other investigators, indicate that under developed-turbulence conditions above the steppe, the turbulent heat flow usually diminishes with increasing height and passes through zero at a height of the order of several hundred meters (see Fig. 6, which shows the mean profile q(z) constructed from

the data of nine aircraft soundings on clear days over the steppe). It may be assumed that this change in heat flow with altitude is determined primarily by the influence of the temperature-field unsteadiness associated with the presence of the regular "diurnal periodicity"; this hypothesis is also consistent with the preliminary results of Telford and Warner [74], who estimated for one particular measurement of the profile q(z) that the variation of q in the layer from z = 16 m up to z = = 320 m is about two-thirds explained by the effect of unsteadiness and the remaining third by the effect of the horizontal meteorological-field nonuniformity.

References

1. A.S. Monin and A.M. Yaglom. Statisticheskaya gidromekhanika (Statistical hydromechanics), Part 1. Izd-vo "Nauka", 1965.

2. A.N. Kolmogorov. Lokal'naya struktura turbulentnosti v neszhimayemoy vyazkoy zhidkosti pri ochen' bol'shikh chislakh Reynol'dsa (Local structure of turbulence in an incompressible viscous fluid at very high Reynolds numbers), Dokl. AN SSSR, 1941, 30, 299-303.

3. G.K. Batchelor. The Theory of Homogeneous Turbulence. Cambridge University Press, 1953.

4. A.M. Yaglom. Nekotoryye klassy sluchaynykh poley v n-mernom prostranstve, rodstvennyye statsionarnym sluchaynym protsessam (Certain classes of stochastic fields in n-dimensional space related to stationary random processes), Teoriya veroyatnostey i yeye primeneniya, 1957, 2, 292-337.

5. A.S. Monin. Struktura atmosfernoy turbulentnosti (The structure of atmospheric turbulence) Teoriya veroyatnostey i yeye primeneniya, 1958, 3, 286-317.

6. A.N. Kolmogorov. Rasseyaniye energii pri lokal'no izotropnoy turbulentnosti (Dissipation of energy in locally isotropic turbulence), Dokl. AN SSSR, 1941, 32, 19-21.

7. G.I. Taylor. The Spectrum of Turbulence. Proc. Roy. Soc., 1938, A164, 476-490.

8. A. Favre, J. Gaviglio and R. Dumas. Quelques mesures de correlation dans le temps et l'espace en soufflerie (Time and space correlation measurements in the wind tunnel), La Rech. Aero., 1952, N. 32, 21-28.

9. R.J. Taylor. Some Observations of Wind Velocity Autocorrelation in the Lowest Layers of the Atmosphere. Austr. J. Phys., 1955, 8, 535-544.

10. H.A. Panofsky, H.E. Cramer and V.R.K. Rao. The Relation Between Eulerian Time and Space Spectra. Quart. J. Roy. Meteorol.

Soc., 1958, 84, 270-274.

11. F. Gifford, Jr. A Simultaneous Lagrangian-Eulerian Turbulence Experiment. Month. Weath. Rev., 1955, 83, 293-301.

12. E.E. Gossard. Power Spectra of Temperature, Humidity and Refractive Index from Aircraft and Tethered Balloon Measurements. IRE Trans. on Antennas and Propogation, 1960, AP-8, 186-201.

13. U.O. Lappe and B. Davidson. On the Range of Validity of Taylor's Hypothesis and the Kolmogorov Spectral Law. J. Atm. Sci., 1963, 20, 569-576.

14. L.R. Tsvang. Nekotoryye kharakteristiki spektrov temperaturnykh pul'satsiy v pogranichnom sloye atmosfery (Certain characteristics of temperature-pulsation spectra in the ground layer of the atmosphere), Izv. AN SSSR, seriya geofiz., 1963, No. 10, 1594-1600.

15. B.M. Koprov and L.R. Tsvang. Pryamyye izmereniya turbulentnogo potoka tepla s borta samoleta (Direct measurements of turbulent heat flow from aboard an aircraft),Izv. AN SSSR, Fizika atmosfery i okeana, 1965, 1, 643-647.

16. A.M. Obukhov. Kharakteristika mikrostruktury vetra v prizemnom sloye atmosfery (Characteristics of wind microstructure in the ground layer of the atmosphere), Izv. AN SSSR, ser. geofiz., 1951, No. 3, 49-68.

17. P.B. MacCready. Atmospheric Turbulence Measurements and Analysis. J. Meteorol., 1953, 10, 325-337.

18. P.B. MacCready. Turbulence Measurements by Sailplane. J. Geophys. Res., 1962, 67, 1041-1050.

19. P.B. MacCready. The Inertial Subrange of Atmospheric Turbulence. J. Geophys. Res., 1962, 67, 1051-1059.

20. J.A. Businger and V.E. Soumi. Variance Spectra of the Vertical Wind Component Derived from Observations with the Sonic Anemometer at O'Neill, Nebraska, in 1953. Arch. Meteorol. Geophys. Bioklimatol., 1958, A10, 415-425.

21. A.S. Gurvich. Eksperimental'noye issledovaniye chastotnykh spektrov i funktsiy raspredeleniya vertikal'noy komponenty skorosti vetra (Experimental investigation of frequency spectra and distribution functions of vertical wind speed component), Izv. AN SSSR, seriya geofiz., 1960, No. 7, 1042-1055.

22. S.L. Zubkovskiy. Chastotnyye spektry pul'satsiy gorizontal'noy komponenty skorosti vetra v prizemnom sloye vozdukha (Frequency spectra of pulsations of horizontal wind speed component in the ground layer of air), Izv. AN SSSR, seriya geofiz., 1962, No. 10, 1425-1433.

23. S.L. Zubkovskiy. Eksperimental'noye issledovaniye spektrov pul'satsiy vertikal'noy komponenty skorosti vetra v svobodnoy atmosfere (Experimental investigation of vertical wind speed component pulsation spectra in the free atmosphere), Izv. AN SSSR, seriya geofiz., 1963, No. 8, 1285-1288.

24. S. Pond, R.W. Stewart and R.W. Burling. Turbulence Spectra in the Wind over Waves. J. Atm. Sci., 1963, 20, 319-324.

25. B.M. Koprov. Spektry turbulentnykh pul'satsiy vertikal'noy komponenty skorosti vetra v pogranichnom sloye atmosfery v usloviyakh razvitoy konvektsii (Turbulent-pulsation spectra of vertical wind component in the boundary layer of the atmosphere under conditions of developed convection), Izv. AN SSSR, Fizika atsmosfery i okeana, 1965, 1, 1151-1159.

26. A.B. Burns. Power Spectra of Low Level Atmospheric Turbulence Measured from the Aircraft. Aeronaut. Res. Council Current Papers, 1964, No. 733.

27. H.L. Grant, R.W. Stewart and A. Moilliet. Turbulence Spectra from a Tidal Channel. J. Fluid Mech., 1962, 12, 241-268.

28. M.M. Gibson. Spectra of Turbulence in a Round Jet. J. Fluid Mech., 1963, 15, 161-173.

29. C.H. Gibson and W.H. Schwartz. The Universal Equilibrium Spectra of Turbulent Velocity and Scalar Fields. J. Fluid Mech., 1963, 16, 365-384.

30. A.S. Gurvich. Izmereniye koeffitsienta asimmetrii raspredeleniya raznosti skorostey v prizemnom sloye atmosfery (Measurement of coefficient of skewness of velocity-difference distribution in the ground layer of the atmosphere), Dokl. AN SSSR, 1960, 134, 1073-1075.

31. R.U. Styuart. O soglasovanii imeyushchikhsya dannykh o spektry i asimmetrii lokal'no izotropnoy turbulentnosti (On the agreement between available data on the spectrum and skewness of locally isotropic turbulence), Dokl. AN SSSR, 1963, 152, 324-326.

32. R.J. Taylor. The Dissipation of Kinetic Energy in the Lowest Layer of the Atmosphere. Quart. J. Roy. Meteorol. Soc., 1952, 78, 179-185.

33. K. Takeuchi. On the Nondimensional Rate of Dissipation of Turbulent Energy in the Surface Boundary Layer. J. Meteorol. Soc. Japan. 1962, 40, 127-135.

34. F. Gifford. Relative Atmospheric Diffusion of Smoke Puffs. J. Meteorol., 1957, 14, 410-414.

35. F. Gifford. Further Data on Relative Atmospheric Diffusion. J. Meteorol., 1957, 14, 475-476.

36. F.K. Ball. Viscous Dissipation in the Atmosphere. J. Meteorol., 1961, 18, 553-557.

37. V.N. Ivanov. Dissipatsiya turbulentnoy energii v atmosfere (Dissipation of turbulent energy in the atmosphere), Izv. AN SSSR, Seriya geofiz., 1962, No. 9, 1261-1267.

38. E.M. Wilkins. Decay Rates for Turbulent Energy Throughout the Atmosphere. J. Atm. Sci., 1963, 20, 473-476.

39. V.N. Ivanov. Turbulentnaya energiya i yeye dissipatsiya v nizhnem sloye atmosfery (Turbulent energy and its dissipation in the lower layer of the atmosphere), Izv. AN SSSR, seriya geofiz., 1964, No. 8, 1405-1413.

40. P. Frenzen. Determination of Turbulent Dissipation by Eulerian Variance Analysis. Quart. J. Roy. Meteorol. Soc., 1965, 91, 28-34.

41. A.S. Monin and A.M. Obukhov. Osnovnyye zakonomernosti turbulentnogo peremeshivaniya v prizemnom sloye vozdukha (Basic relationships in turbulent agitation in the ground layer of air), Trudy geofiz. in-ta, 1954, No. 24 (151), 163-187.

42. B.M. Koprov and L.R. Tsvang. Melkomasshtabnyye kharakteristiki polya temperatury i vetra v stratifitsirovannom pogranichnom sloye (Small-scale characteristics of temperature and wind field in a stratified boundary layer), Izv. AN SSSR, Fizika atmosfery i okeana, 1966, 2, 1142-1150.

43. A.M. Obukhov. Struktura temperaturnogo polya v turbulentnom potoke (Structure of the temperature field in a turbulent flow), Izv. AN SSSR, seriya geogr. i geofiz., 1949, 13, 58-69.

44. S. Corrsin. On the Spectrum of Isotropic Temperature Fluctuations in an Isotropic Turbulence. J. Appl. Phys., 1951, 22, 469-473.

45. S.I. Krechmer. Issledovaniya mikropul'satsiy temperaturnogo polya v atmosfere (Investigation of temperature-field micropulsations in the atmosphere), Dokl. AN SSSR, 1952, 84, 55-58.

46. M. Shiotani. On the Fluctuation of the Temperature and Turbulent Structure near the Ground. J. Meteorol. Soc. Japan, 1955, 33, 117-123.

47. V.I. Tatarskiy. Mikrostruktura temperaturnogo polya v prizemnom sloye vozdukha (Microstructure of temperature field in the ground layer of air), Izv. AN SSSR, Seriya geofiz., 1960, No. 11, 1674-1678.

48. L.R. Tsvang. Izmereniya chastotnykh spectrov temperaturnykh pul'satsiy v prizemnom sloye atmosfery (Measurements of temperature-pulsation frequency spectra in the ground layer of the atmosphere), Izv. AN SSSR, seriya geofiz., 1960, No. 8, 1252-1262.

49. L.R. Tsvang. Izmereniya spektrov temperaturnykh pul'satsiy v svobodnoy atmosfere (Measurements of temperature-pulsation spectra in the free atmosphere), Izv. AN SSSR, seriya geofiz., 1960, No. 11, 1674-1678.

50. A.S. Gurvich and T.K. Kravchenko. O chastotnom spektre pul'satsiy temperatury v oblasti melkikh masshtabov (Frequency spectrum of temperature pulsations in the small-scale range), Trudy in-ta fiziki atmosfery AN SSSR, 1962, No. 4, 144-146.

51. S. Pond. Turbulence Spectra in the Atmospheric Boundary Layer over the Sea. Ph. Thesis; Institute of Oceanogr., Univ. British Columbia, Vancouver, 1965.

52. A.S. Gurvich and S.L. Zubkovskiy. Ob otsenke strukturnoy kharakteristiki pul'satsiy temperatury v atmosfere (Estimation of the structure characteristic of temperature pulsations in the atmosphere), Izv. AN SSSR. fiziki atmosfery i okeana, 1966, 2, 202-204.

53. A.M. Yaglom. O lokal'noy strukture polya temperatur v turbulentnom potoke (Local structure of temperature field in turbulent flow), Dokl. AN SSSR, 1949, 69, 743-746.

54. A.M. Obukhov. O strukture temperaturnogo polya i polya skorostey v usloviyakh svobodnoy konvektsii (Structure of the temperature and velocity fields under the conditions of free convection), Izv. AN SSSR, seriya geofiz., 1960, No. 9, 1392-1396.

55. Y.H. Pao. Structure of Turbulent Velocity and Scalar Fields at Large Wave Number. Phys. Fluids, 1965, 8, 1063-1075.

56. Ye.A. Novikov. O spektre energii turbulentnogo potoka neszhimayemoy zhidkosti (Energy spectrum of turbulent flow of an incompressible fluid), Dokl. AN SSSR, 1961, 139, 331-334.

57. P.G. Saffman. On the Fine-Scale Structure of Vector Fields Convected by a Turbulent Fluid. J. Fluid Mech., 1963, 16, 545-572.

58. N.F. Gorshkov. Ob energeticheskom spektre turbulentnosti v oblasti bol'shikh volnovykh chisel (Energy spectrum of turbulence in the range of large wave numbers), Izv. AN SSSR, Fizika atmosfery i okeana, 1966, 2, 989-992.

59. G.K. Batchelor. Small-Scale Variation of Convected Quantities like Temperature in Turbulent Fluid. Part I. General Discussion and the Case of Small Conductivity. J. Fluid Mech., 1959,

5, 113-133.

60. G.K. Batchelor, I.D. Howells and A.A. Townsend. Small-Scale Variation of Convected Quantities like Temperature in Turbulent Fluid. Part II. The Case of Large Conductivity. J. Fluid Mech., 1959, 5, 134-139.

61. Ye.A. Novikov. O fluktuatsiyakh elektronnoy plotnosti v ionosfere (Electron-density fluctuations in the ionosphere), Dokl. AN SSSR, 1961, 139, 587-589.

62. F. Gifford. The Interpretation of Meteorological Spectra and Correlations. J. Meteorol., 1959, 16, 344-346.

63. A.M. Obukhov. O vliyanii arkhimedovykh sil na strukturu temperaturnogo polya v turbulentnom potoke (Influence of Archimedean forces on the structure of the temperature field in turbulent flow), Dokl. AN SSSR, 1959, 125, 1246-1248.

64. R. Bolgiano. Turbulent Spectra in a Stable Stratified Atmosphere. J. Geophys. Res., 1959, 64, 2226-2229.

65. J.L. Lumley and H.A. Panofsky. The Structure of Atmospheric Turbulence. Interscience Publ., N.Y.-London-Sydney, 1964.

66. N. Thompson. Intensities and Spectra of Vertical Wind Fluctuations at Heights Between 100 and 500 ft. in Neutral and Unstable Conditions. Quart. J. Roy. Meteorol. Soc., 1962, 88, 328-334.

67. S. Berman. Estimating the Longitudinal Wind Spectrum near the Ground. Quart. J. Roy. Meteorol. Soc., 1965, 91, 302-317.

68. R.N. Swanson and H.E. Cramer. A Study of Lateral and Longitudinal Intensities of Turbulence. J. Appl. Meteorol., 1965, 4, 409-417.

69. N.L. Byzova, V.N. Ivanov and S.A. Morozov. Turbulentnyye kharakteristiki skorosti vetra i temperatury v pogranichnom sloye atmosfery (Turbulent characteristics of wind speed and temperature in the boundary layer of the atmosphere), This collection, pp. 32-53.

70. V.N. Kolesnikova and A.S. Monin. O spektrakh kolebaniy meteorologicheskikh poley (The spectra of meteorological-field oscillations), Izv. AN SSSR, fizika atmosfery i okeana, 1965, 1, 653-669.

71. A.S. Gurvich. O spektrakh vertikal'nykh turbulentnykh potokov v prizemnoy sloye atmosfery (The spectra of vertical turbulent flows in the ground layer of the atmosphere), Izv. AN SSSR, Fizika atmosfery i okeana, 1965, 1, 764-766.

72. A.F. Bunker. Heat and Water-Vapor Fluxes in Air Flowing Southward over the Western North Atlantic Ocean. J. Meteorol., 1960, 17, 52-63.

73. J.W. Telford and J. Warner. Fluxes of Heat and Vapor in the Lower Atmosphere Derived from Aircraft Observations. J. Atm. Sci., 1964, 21, 539-548.

74. J. Warner and J.W. Telford. A Check of Aircraft Measurements of Vertical Heat Flux. J. Atm. Sci., 1965, 22, 463-465.

Discussion

Ye. Inoue – Is there a scale that characterizes the dimension of the smallest perturbations and is the same for the cases of velocity and the temperature fluctuations?

A.M. Yaglom – Since the Prandtl number for air is of the order of unity, the dimensions of the smallest velocity and temperature perturbations should be of the same order. However, direct empirical data on the boundary of the inertial (or, more precisely, convective) range of the temperature-pulsation spectrum at the small-scale end are as yet, unfortunately, lacking.

O.M. Phillips – In estimating the rate of energy dissipation from the measured value of the vertical-velocity spectrum for a given k, were you able to verify that the value that you selected fell in the inertial subrange in all cases?

A.M. Yaglom – Yes, we were. Over more than two years, we made a great many measurements of spectra over a broad range of wave numbers and thoroughly studied the question as to the wave numbers at which the appearance of deviations from the "5/3 law" can be expected. Only then did we go on to determine $\bar{\varepsilon}$ from the spectrum for one k.

V.N. Ivanov – The largest nonuniformity dimension for which the "5/3 law" is valid is found in many cases to be considerably greater than the height of the observation. What determines the external turbulence scale in these cases?

A.M. Yaglom – Usually, one-dimensional spectra are measured. The deviation from the "5/3 law" begins to manifest for one-dimensional spectra approximately one order later than for three-dimensional spectra. But if, as is physically more natural, we take the external scale to mean the length defining the boundary of the inertial subrange for the three-dimensional spectrum, then this external scale will probably not exceed the distance to the ground in the ground layer.

[English Summary]

The purpose of this survey is to consider some past and current empirical data on first and second moments of turbulent fluctuations in the atmospheric boundary layer and to compare them with some theoretical deductions.

Major attention is given to the double-point second order moments. The most general moment of this type is the space-time crosscorrelation of two meteorological fields a (x, t) and b (x, t) defined by eq. (1) on p. 30. In order to reveal the contribution of the small-scale pulsations it is convenient to use a moving coordinate system and to consider, instead of the correlation functions, the structure functions of the type (2) and (3). Another general method of obtaining small-scale characteristics makes use of Fourier transformations and considers, instead of correlation functions, either the space-time spectra F_{ab} (k, ω) of eq. (4), or space spectra F_{ab} (k) = F_{ab} (k, 0), or time spectra F_{ab} (ω) = F_{ab} (0, ω). When the wave number k and the frequency ω are sufficiently great the spectra evidently are the small-scale characteristics. Time spectra are easiest to define experimentally; moreover the aircraft measurements make it also possible to define with good precision the one-demensional space spectra $F^{(1)}_{ab}$ (k) in the direction of aircraft motion.

The measurement of time spectra has the drawback that from the theoretical point of view temporal statistical characteristics are more complicated than purely spatial characteristics. In order to obtain the space characteristics from the time ones, usually Taylor's hypothesis about «frozen» pattern of turbulence is used. The equations (5) (or (5')) and (6) where $F^{(1)}_{ab}$ (k) is a one-dimensional space spectrum in the mean-wind direction result from Taylor's hypothesis. The most convenient method of verification of this hypothesis for the atmosphere is the comparison of measurements made from an aircraft flying at a constant height with great speed with simultaneous measurements of time characteristics at the same height made from a captive balloon or a tower. The results of such a verification can be found in references [11 to 15]; they show that the pattern of atmospheric turbulence can be considered as «frozen» for a wide range of scales. Fig. 1 illustrates the results of such a verification of eq. (6) for the spectra $F^{(1)}_{ww}$(k) and $F^{(1)}_{TT}$ (k) of vertical velocity and temperature made at field station of the Institute of Atmospheric Physics near Tsimlansk. They show that the range of applicability of Taylor's hypothesis to the atmosphere is even greater than expected.

Most of the observational data are collected in the form of time spectra of fluctuations of different meteorological variables, which, with the help of Taylor's hypothesis, can be transformed to one-dimensional space spectra in the direction of the mean wind. The well-known Kolmogorov theory of locally isotropic turbulence asserts that the one-dimensional spectra $F^{(1)}_{uu}$ (k), $F^{(1)}_{vv}$ (k), and $F^{(1)}_{ww}$ (k) of horizontal, lateral, and vertical components of wind as well as three-dimensional wind spectrum E (k) must satisfy the universal «5/3 laws» (see eq. (7)) in the inertial subrange. Similarly the structure functions must satisfy the universal «2/3 laws» (9) in the inertial subrange. The numerical coefficients in the equations (7) and (9) are connected by means of conditions (8) and (10).

The observational data of references [9] and [16 to 26] show that the «5/3 laws» and «2/3 laws» are satisfied in the atmosphere with good precision (cf. also Fig. 1 and Fig. 5). The data of simultaneous measurements of spectra $F^{(1)}_{uu}$ (k) and $F^{(1)}_{ww}$ (k) at the Institute of Atmospheric Physics indicate also good agreement with the theoretical result $C_1/C_1' = 0.75$ of eq. (8). The data of the last few years have allowed, at least, determination of the value of C_1 with 10—15% accuracy; namely $C_1 \approx 0.45$—0.5 (cf. [31]).

If we assume the numerical coefficients in the «5/3 laws» to be known, then in order to determine the velocity spectra in the inertial subrange we only need to know the value of mean rate of energy dissipation $\bar{\varepsilon}$. At present we know several different methods for determining $\bar{\varepsilon}$ and there are many published data on its measurements in the atmosphere (see, e.g., [16, 17, 19, 22, 23, 25] and [32 to 40]). However the results obtained are till now in some cases contradictory, often have insufficient accuracy, and are still rather incomplete. At the Institute of Atmospheric Physics the values $\bar{\varepsilon}$ were determined systematically during several summers over the steppe by mast, tower, and aircraft measurements of spectrum $F_{ww}^{(1)}(k)$ at one wave number k in the inertial subrange. The results show that the vertical profiles of $\bar{\varepsilon}$ have different forms at different times of the day and under different meteorological conditions, that is, the profile $\bar{\varepsilon}(z)$ depends significantly on thermal stratification. The typical forms of the profile $\bar{\varepsilon}(z)$ at midday in the anticyclonal summer weather (i. e. in the conditions of developed convection), in the early morning (in conditions of developing convection), and in the evening (in conditions of almost neutral stratification) are shown in Fig. 2.

The «2/3 law» and the «5/3 law» for the temperature (or for any other passive and conserved scalar quantity) were obtained theoretically in references [43, 44, 53]. According to these laws the equations (12), (13) and (14) must be valid in the inertial subrange where $\bar{\varepsilon}_T = \chi \sum_i \left(\overline{\frac{dT}{dx_i}}\right)^2$ is the mean rate of «temperature dissipation» (χ is the coefficient of thermal conductivity). The empirical data confirming the applicability of the laws to the atmosphere can be found, e. g. in references [45 to 51]. There are several different methods of estimation of the numerical coefficients in the laws (12) and (13). The obtained estimations show considerable discrepancies; however the most reliable among them make us think that $A_T \approx 2.8$ and $C_T' \approx 0.7$.

The measurements of the temperature spectrum in the inertial subrange give the possibility to determine the value of the dimensional quantity $B_T = A_T \bar{\varepsilon}_T \bar{\varepsilon}^{-1/3}$. Fig. 3 shows the typical profiles of the quantity B_T in summer conditions over the steppe at different times of the day (at midday, in the morning, and in the evening). The profiles were obtained at the Institute of Atmospheric Physics by means of aircraft measurements of temperature spectrum $F_{TT}^{(1)}(k)$. They show that in conditions of developed convection B_T decreases with height approximately proportional to $z^{-1/3}$ in a thick layer. The profiles of B_T depend mostly on the profile of mean temperature gradient $\frac{d\overline{T}}{dz}$; this can be seen e. g. from Fig. 4 showing the dependence of B_T on $\frac{d\overline{T}}{dz} + \gamma_a = \gamma + \gamma_a$ (where γ_a is the adiabatic temperature gradient) in morning hours.

In the highest wave number range, comparable with or even exceeding the so-called Kolmogorov wave number $k^* = 1/\eta = \nu^{-1/4} \cdot \bar{\varepsilon}^{1/4}$, the spectra $E(k)$, $F_{uu}^{(1)}(k)$, and $F_{ww}^{(1)}(k)$ depend on molecular viscosity and have the forms (16) where $\varphi_1(x)$, $\varphi_2(x)$ and $\varphi_3(x)$ are the universal functions. According to empirical data of [24] and [27] the functions $\varphi_l(x)$, $l = 1, 2, 3$, begin to deviate from the constants, C, C_1, and C_1' approximately at $x \approx 1/8$. At present we have almost no data on the values of the universal functions in the range $x > 1$. However it is possible to recommend as a purely preliminary approximation Gorshkov equation (18) for $\varphi_2(x)$. This equation argees rather well with the observational data of Grant, Stewart and Moilliet [27] (see Fig.5) and with the theoretical result of Novikov [56] concerning the asymptotic behaviour of velocity spectra in the range $k \gg k^*$.

In the range of small wave numbers, or great scales, the turbulent fluctuations become nonisotropic. The nonisotropic fluctuations determine different typical scales of turbulent inhomogeneities, the magnitudes of turbulent pulsations (i. e. the variances of the meteorological fields), and single-point cross correlations between different meteorological fields (the most important of such cross correlations are the turbulent fluxes). Some empirical and theoretical results concerning these nonisotropical characteristics can be found in references [63 to 74]. In the last section of the survey the discussion of some problems of the investigation of such characteristics is given.

TURBULENCE CHARACTERISTICS OF WIND SPEED AND TEMPERATURE IN THE BOUNDARY LAYER OF THE ATMOSPHERE

N.L. Byzova, V.N. Ivanov,
and S.A. Morozov

Institute of Applied Geophsics
Obninsk, USSR

Study of turbulent motions in the atmospheric boundary layer not only pursues the goal of refining existing boundary-layer theories and solving a number of applied problems, but is also of a certain interest from the standpoint of study of turbulence itself in stratified flow with shear at large Reynolds numbers. Like most research in the field of atmospheric turbulence, it is basically at the level of accumulating and refining experimental facts. The present paper is devoted to the results of experimental studies carried out on the 300-meter meteorological mast of the Applied Geophysics Institute.

1. WIND SPEED SPECTRA IN THE INFRALOW FREQUENCY RANGE

Among the first problems that arise in study of turbulence in the atmosphere is that of estimating the range of scales that this motion encompasses. The least-studied range of the spectrum is its low-frequency part, which is associated with the largest vortices that arise in the boundary layer. Interest attaches to improvement of data on the spectral-density minimum that separates the turbulent and mesometeorological segments of the spectrum (van der Hoven [11], Panofsky and Deland [9], Monin and Kolesnikova [4]). The spectral density S(f) was obtained

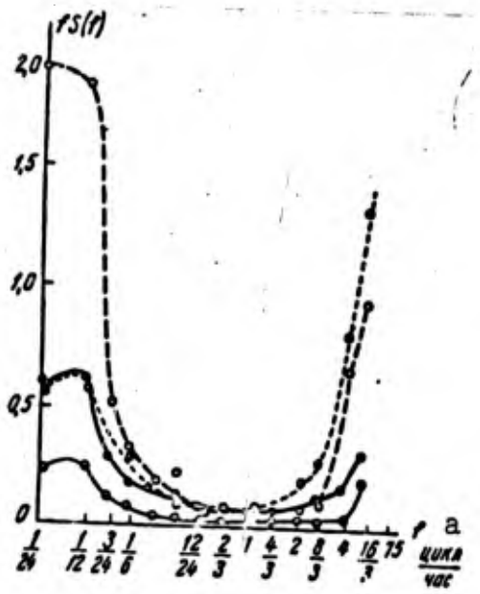

Fig. 1. Spectral density of longitudinal wind speed component in infra-low frequency range at 25, 75, 150 and 300-m levels (the units on the axes of ordinates are arbitrary).
KEY: (a) cycles/h.

from data on the longitudinal wind-speed component measured on the 300-meter meteorological mast in January 1965 (in 400 h of continuous observation). Spectra were taken for four levels, 25, 75, 150, and 300 m, in the frequency range from 0.04 to 5 periods/h. The calculations were made on an electronic computer. The data obtained are presented in Fig. 1 in the coordinates f and $fS(f)$, where f is the frequency. We see that the energy distribution is this frequency range has a distinct minimum, which separates the turbulent and mesometeorological region of the spectrum. At the lower levels, the minimum falls at frequencies of 0.15-4 periods/h, but at 0.15-2 cycles/h at the higher levels. The results obtained also confirm the presence of a semidiurnal maximum in the spectral densities, coinciding with the similar peak of the function $S(f)$ at these frequencies that was cited in [11]. The spectral density at the minimum is 5-10% of this maximum.

The averaged low-frequency boundary of the turbulent range can be estimated from the spectral densities pertaining to various heights: for low levels it is 5 periods/h and for higher levels about 3 periods/h. The horizontal dimensions of the vortices corresponding to these frequencies are of the order of several kilometers, or considerably in excess of the thickness of the atmospheric boundary layer.

We note that the spectral densities given here pertain to the winter period, when there were no conspicuous convective conditions. However, comparison of these data with data obtained for summer at 100 m (Panofsky and Deland [9]) shows no fundamental differences between them.

2. TURBULENT ENERGY OF THE LONGITUDINAL WIND SPEED COMPONENT

These estimates of the low-frequency boundary of the turbulent range enable us to select the frequency band needed to determine the turbulent energy of the longitudinal wind-speed component $\overline{u'^2}$. For conditions that exclude strong convection, as we showed above, it is limited to frequencies of 3-5 periods/h. To permit measurements under convective conditions as well, a specialized analog-type apparatus was built for the frequency range to 1 period/h. Practice showed that it was generally sufficient to use the narrower band to 2 periods/h. The instrument

averaged the output quantities over a time of 100 s, and then the averaging period was raised to 1-2 h in the process of analyzing the material obtained.

The longitudinal velocity component was measured with propeller-type sensors mounted at 10 levels in the lower 300-meter layer, including stations in the ground layer at the 2- and 8-m levels. The ground-layer sensors were set up at a distance of 200 m from the main mast. The transducer spatial averaging due to inertia was 4 m, and the transducer signal was averaged with an additional time constant of 0.5 s. The corresponding estimates indicated that such averaging introduces no substantial error into the turbulent-energy value at moderate wind speeds at heights of 25 m and up.

As we know, it is most convenient to present the turbulent energy $\overline{u'^2}$ in the form of the dimensionless ratio $\sqrt{\overline{u'^2}}/u$, where u is the velocity of the unperturbed flow. In our case, it would have been convenient to use the geostrophic wind speed u_g as this quantity. However, we did not have systematic measurements of u_g over the entire time of the observations, so that the value u_{300} of the wind speed at a height of 300 m was used as an estimate of u_g. The degree to which this substitution is justified can be judged from the data given in [1].

To bring out the nature of the turbulent-energy variation with time over the entire layer, it is helpful to represent the results obtained in the form of lines of equal turbulence intensity. Such data are shown in Fig. 2, as obtained during the day 28 April 1965.

During this day, the temperature stratification was close to indifferent. From 01 to 08 hours, we observed very weak stability (average deviation from the dry adiabatic gradient -0.15° over 100 m). After 11 hours, the temperature gradient in the bottom of the layer was 1°/100 m. The wind speed was stable to 09 hours, at 7-8 m/s at the 300-m height; after 11 hours it gradually decreased to 5-6 m/s, and by 14 hours it had fallen to 4 m/s.

An increase in turbulence intensity was observed during the day despite the very indistinct change in stratification. The turbulence-intensity field is characteristically somewhat mottled, an effect that we attribute primarily to the existence of large-scale inhomogeneities that make it impossible to obtain statistically stable values for the wind-speed dispersion over the time in question. The variation of $\sqrt{\overline{u'^2}}/u_{300}$ with time for the most part follows the variation of atmospheric state, although this conformity is incomplete: for example, after 16 hours, the temperature gradient became somewhat steeper than adiabatic, but the turbulence intensity decreased, following the decrease in wind speed.

Apart from the time variations, interest attached to examination of the turbulent-energy intensity profiles $\sqrt{\overline{u'^2}}/u_{300}$ for

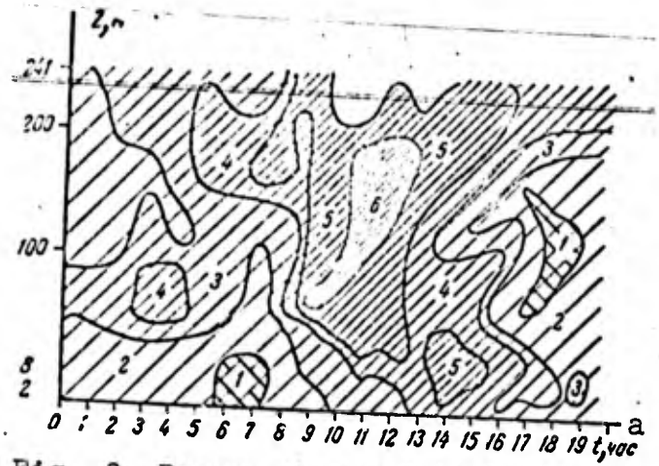

Fig. 2. Range of equal turbulence intensities $\sqrt{u'^2}/u_{300}$ according to measurements on 28 April 1965.

1 — ≤ 0.05; 2 — 0.05—0.08; 3—0.08—0.1; 4 — 0.01—0.12; 5 — 0.12 — 0.14; 6 — ≥ 0.14

KEY: (a) hours.

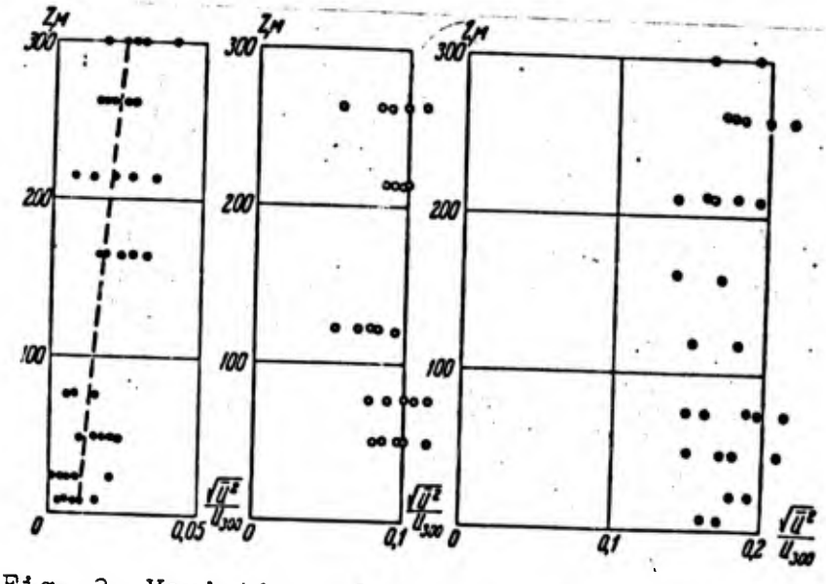

Fig. 3. Variation of turbulence intensity $\sqrt{u'^2}/u_{300}$ with height for various stratifications. ●) weak stability; o) indifferent equilibrium; ⊖) moderate convection.

various stratifications in the layer being studied (Fig. 3). We recall that turbulent energy was measured in the frequency range to 2 periods/h, with each $\sqrt{u'^2}$ value determined from six ten-minute profiles. The profiles obtained cover three states: weak stability, the indifferent state, and weak inversion. The diagrams show a significant dependence of turbulent-energy intensity

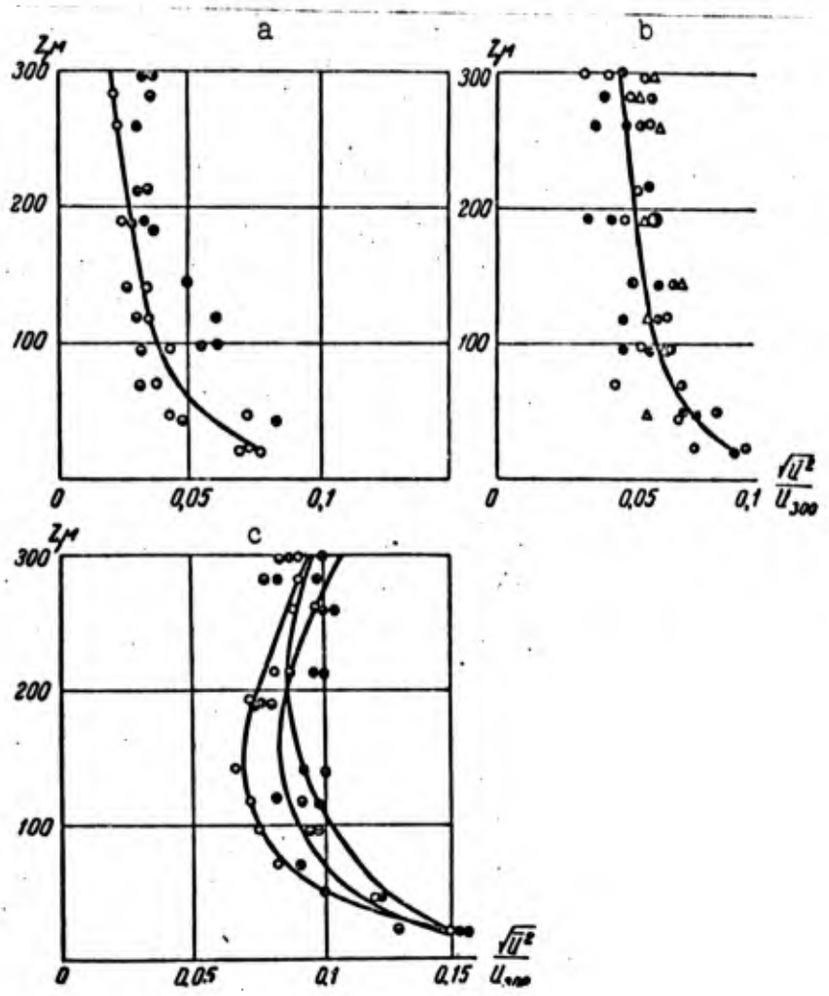

Fig. 4. Variation of turbulent intensity $\sqrt{u'^2}/u_{300}$ with height for limited passband. Group stability parameter $B = \Delta T_{1-4}/u_4^2$: a) +0.0027; b) −0.0005; c) −0.003.

on stratification. We see that under the conditions considered, no decrease in turbulent energy with height is observed, and with stable stratification there is even a tendency for it to increase.

For comparison, let us consider the nature of the height variation of turbulent energy measured in a narrower frequency band — at the low-frequency boundary determined by a 5-minute averaging time (Ivanov [3]). These data are given in Fig. 4. We note that here the range of stratification change is considerably smaller than for the profiles shown in Fig. 3. For conditions of weak convection, we have an increase in turbulent-energy intensity beginning at a height of about 150 m. The first two groups are singular in that turbulent intensity diminishes with altitude. This fact distinguishes the results shown here from those of the broad-band measurements in Fig. 3.

The behavior of turbulent energy for 5-minute averaging is consistent with the familiar notion that it is basically generated in the lower 100-meter layer and determined for states near indifferent equilibrium by the term $\tau(\partial u/\partial z)$ of the turbulent-energy balance equation, where τ is the shear stress. For turbulent-energy profiles obtained with the system passband extending to 2 periods/h, the mechanism set forth above is incomplete. It is apparently necessary here to take account of secondary turbulent-energy-generating sources that give rise to the lower-frequency oscillations with periods longer than 5 min. At a wind speed of 5 m/sec, this corresponds to an eddy size of the order of 1.5 km. Since these dimensions exceed the thickness of the boundary layer, the appearance of these eddies is linked primarily with the horizontal structure of wind speed. In this connection, interest attaches to study of the large-scale inhomogeneities.

3. LARGE-SCALE INHOMOGENEITIES

The large-scale inhomogeneities play an important role in the atmosphere's boundary layer. First of all, they are intermediaries in the transmission of turbulent-flow mean-motion energy. Secondly, like the small-scale motions, they participate in the process of agitating the boundary layer. In this case, however, the agitation process differs from diffusion of the gradient type, which is associated with smaller vortices; it must therefore be considered separately. To ascertain the mechanism of these phenomena, it is necessary to know the spatial structure of these inhomogeneities. Large-scale eddies were investigated in [10, 8] for laboratory conditions. Similar measurements made in the boundary layer of the atmosphere will be of interest.

On the basis of data on the longitudinal wind speed component, measurements of the large-scale inhomogeneities were made at the high meteorological mast of the Applied Geophysics Institute. To describe the statistical properties of the longitudinal component, we used the correlation function

$$R_{uu}(M_0, M_1, -M_0; t_0, \tau) = \frac{\overline{u'(M_0, t_0)\, u'(M_1 - M_0, t_0 + \tau)}}{\left[\overline{u'^2(M_0, t_0)}\ \overline{u'^2(M_1 - M_0, t_1)}\right]^{1/2}}, \qquad (1)$$

where $M_0 = \{x_0, y_0, z_0\}$, $M_1 = \{x_1, y_1, z_1\}$ are points in space (x is the coordinate in the direction of flow and y that across the flow; z is height), t_0 and $t_1 = t_0 + \tau$ are points in time, and u' is the pulsation of the longitudinal velocity component. The available experimental data enabled us to determine only particular cases of the correlation function: 1) the transverse correlation function $R_{uu}(z_0, z; t_0, 0)$, where $z = z_1 - z_0$, 2) the time correlation function $R_{uu}(z_0, 0; t_0, \tau)$ and 3) the space-time correlation function $R_{uu}(z_0, z; t_0, \tau)$.

Measurement of correlation functions in the atmospheric boundary layer in the large-scale range is a more difficult

problem than the analogous wind-tunnel measurements. This is primarily because of the limited time within which the observed process can be regarded as stationary and uniform. Certain difficulties also arise due to the small amplitudes of the large-scale motions. To increase their relative magnitude, we filtered the signals from the speed transducers, thus reducing the energy of the high-frequency components. The transfer function of the filter used had the form

$$\Phi(\omega) = \frac{1}{\sqrt{(\omega\tau_0)^2 + 1}}, \qquad (2)$$

where τ_0 was taken equal to 30 sec. Needless to say, such filtration does not definitely solve the problem of isolating the large-scale inhomogeneities out of the entire set present in turbulent flow, since the relationship between them and the rest of the spectrum depends on wind speed and stratification. However, calculations indicated that it increases the specific weight of these components in the signals studied to a substantial degree.

At the present time, there is no definitive theory of the large-scale inhomogeneities. We can only advance certain considerations regarding the correlation functions listed above. It follows from the continuity equation that for the transverse correlation function

$$\iint R_{uu}(M_0; 0, y, z; t, 0)\, dy\, dz = 0 \qquad (3)$$

(see, for example, [10]). It follows from Formula (3) that there must necessarily be regions in which the correlation function $R_{uu}(M_0, 0, y, z; t, 0)$ is negative. Physically, this means that a counterflow must exist for the velocity pulsations in the transverse flow of the plane. Generally speaking, (3) is valid for the function $R_{uu}(M_0, 0, y, z; 0, 0)$ calculated from the entire frequency spectrum; however, we may expect that the contradiction will arise basically from large-scale nonuniformities comparable with the dimensions of the flow itself and will depend on their structure. An investigation of certain simple similar structures was set forth in [10, 8]. To be able to submit definite judgments as to the shape and orientation of the eddies, it is necessary to know, at the very least, the correlation functions of all three wind-speed components in the three directions. Since we did not have this information, we can offer only certain particular remarks regarding structure.

Experimental data obtained on structure on the high meteorological mast pertain basically to weak stability and moderate convection. The correlation functions $R_{uu}(z_0, z; t_0, 0)$ are shown in Fig. 5 for the inversion state. The functions $R(z_0, z; t_0, 0)$ are characterized in a number of cases by the presence of an intrinsically negative range for z above 100 m. For comparison, we note that according to [8], similar correlation functions for the indifferent state (obtained in the wake behind a cylinder and in the boundary layer on a flat plate)

have no negative region.

The presence of a region of negative $R_{uu}(z_0, z; t_0, 0)$ indicates that the eddy structure for stable stratification has its rotation-axis component in the direction perpendicular to the Oxz plane, something that is not observed in the track behind a cylinder or in the boundary layer on the plate.

The time correlation functions $R_{uu}(z_0, 0; t_0, \tau)$ which pertain to the stable state (Fig. 6), are characterized by a very long correlation time of the order of 10-30 min, which corresponds to inhomogeneity dimensions of the order of 3-10 km. This state is characterized by intrinsically anisotropic inhomogeneities stretched out in the direction of flow.

We note that in a number of cases, the correlation functions $R_{uu}(z_0, 0; t, \tau)$ had the form shown in Fig. 7, which may be regarded as the sum of two correlation functions related by the motions of two different scales [10].

With diminishing stability of the boundary layer and the approach to the indifferent state, the correlation functions $R_{uu}(z_0, z; t_0, 0)$ along the vertical cease to be negative (Fig. 8).

In moderate convection (Fig. 9), we observe a now substantial correlation of the velocity values over the entire layer under consideration. The correlation does not drop below 0.5 here. The $R_{uu}(z_0, 0; t, \tau)$ that correspond to convective conditions (Fig. 10) have a negative region, indicating a definite periodic structure of the inhomogeneities along the horizontal. The characteristic horizontal dimension of the inhomogeneities is of the order of 1 km (the corresponding correlation time is 3-5 min). The anisotropy diminishes substantially in moderate convection. We also observe good homogeneity over the entire height of the layer.

Thus, the data presented confirm that the structures of stable and unstable states are quite different. One of the conclusions to be drawn from this is as follows. For the state of weak stability (Fig. 5), the largest-scale nonuniformities have vertical dimensions not exceeding 50-100 m. Hence the mixing process in the 300-meter vertical layer takes place by gradient diffusion. The situation is different in the unstable state. In this case, the correlation covers the entire 300-meter layer, and the mixing process is determined not only by turbulent diffusion, but also by participation of large eddies in it.

An example of a space-time correlation function appears in Fig. 11, where the lines of equal correlation are shown in the coordinates $\underline{z}$, $\underline{t}$. These results are of the same type as the data for the correlation function in the wake, although they are presented in other coordinates. The picture is not symmetrical: the maximum correlation values lead and lag in time for the upper and lower layers.

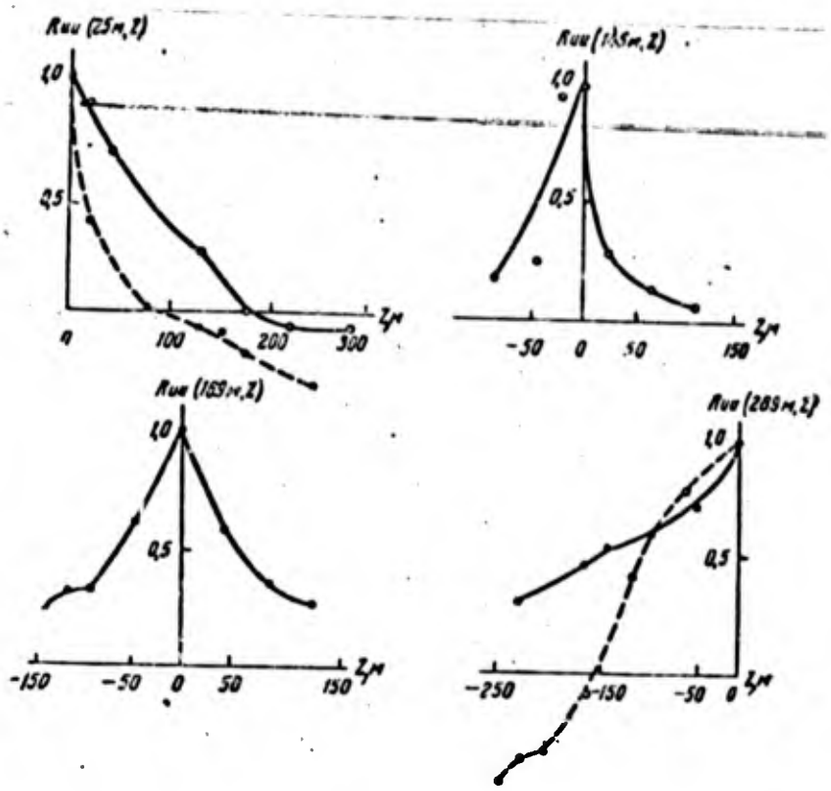

Fig. 5. Correlation functions $R_{uu}(z_0, z; t_0, 0)$ for weak stability (the various symbols pertain to different measurement series).

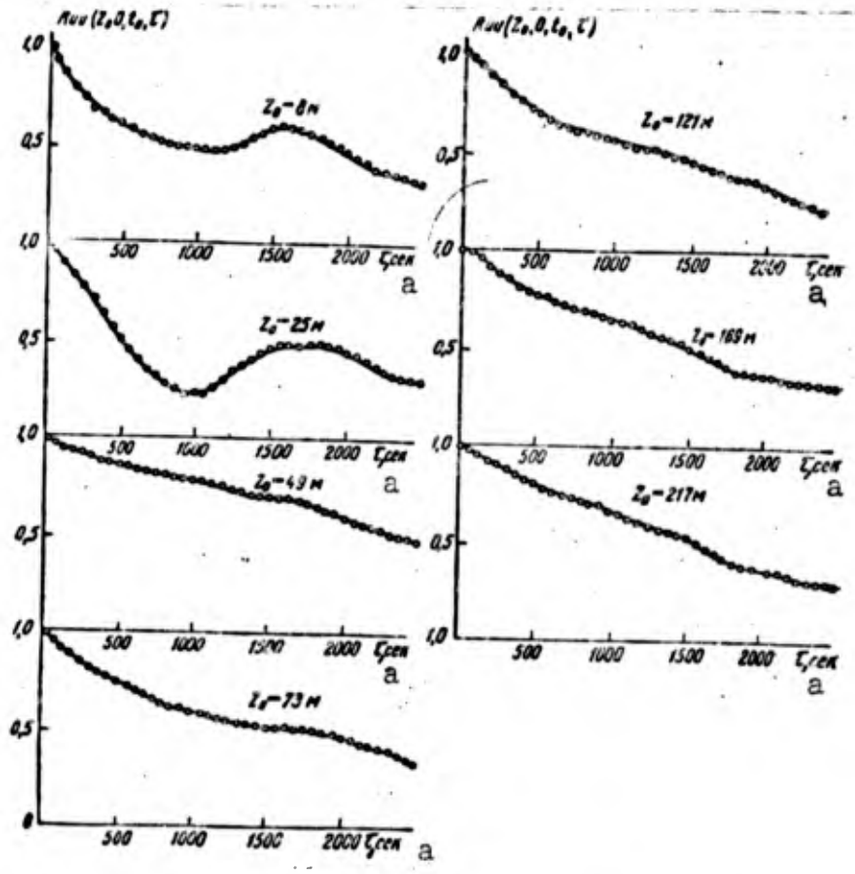

Fig. 6. Time correlation functions $R_{uu}(z_0, 0; t_0, \tau)$ for weak...
KEY: (a) seconds.

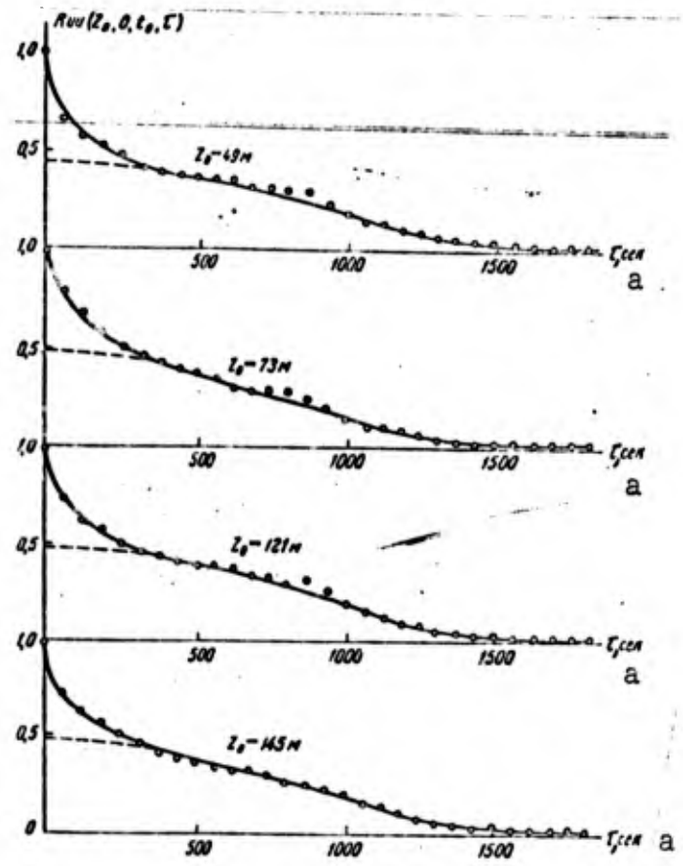

Fig. 7. Time correlation functions $R_{uu}(z_0, 0; t_0, \tau)$ for a nearly indifferent state.
KEY: (a) seconds.

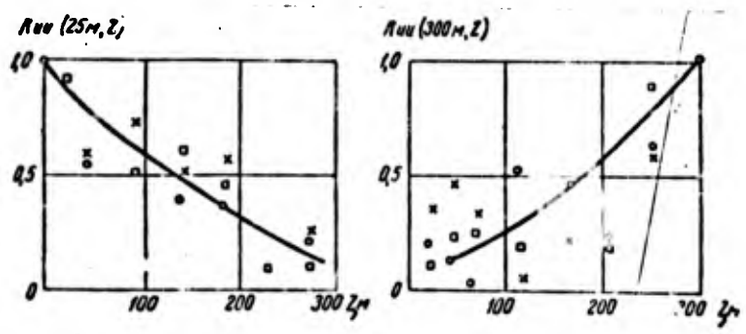

Fig. 8. Correlation functions $R_{uu}(z_0, z, t_0, 0)$ for nearly indifferent states.

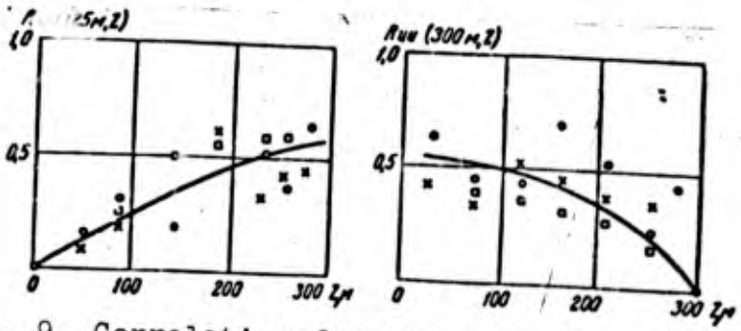

Fig. 9. Correlation functions $R_{uu}(z_0, z; t_0, 0)$ for moderate convection.

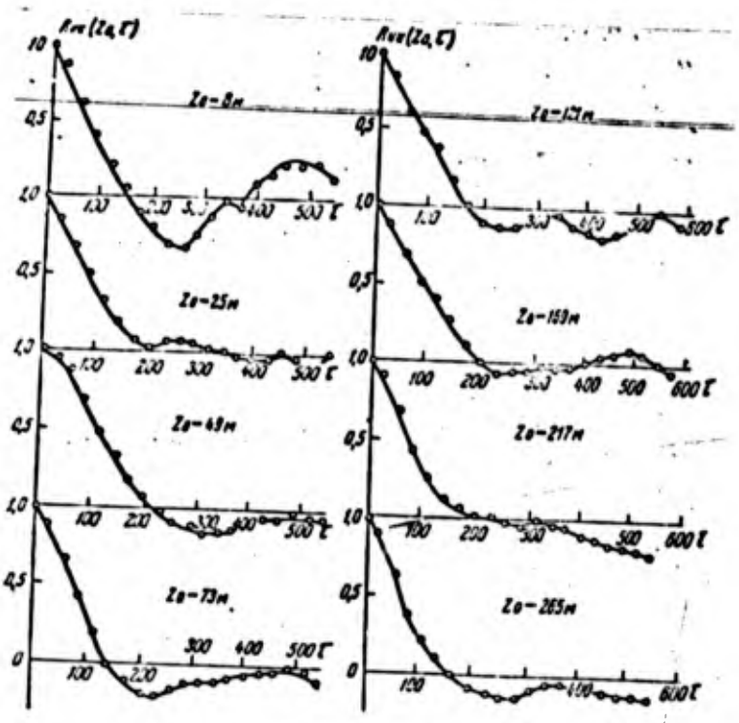

Fig. 10. Time correlation functions $R_{uu}(z_0, 0; t_0, \tau)$ for moderate convection.

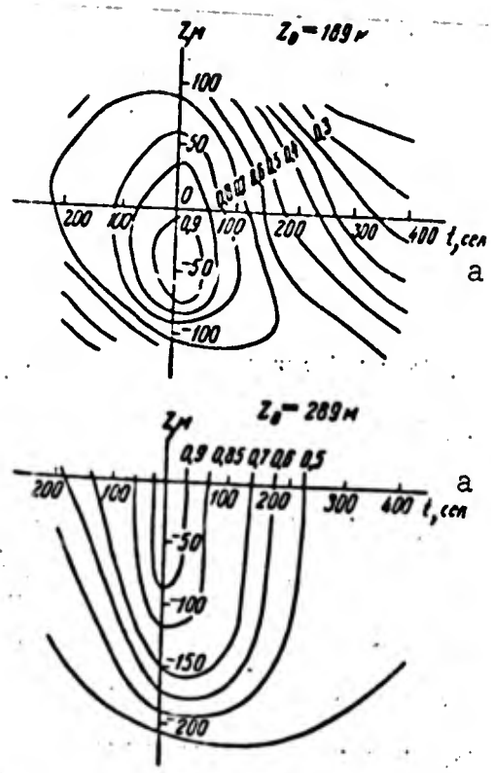

Fig. 11. Lines of equal correlation of the correlation function $R_{uu}(z_0, z; t_0, \tau)$

4. DISSIPATION OF TURBULENT ENERGY

The turbulent energy dissipation $\bar{\varepsilon}$ is a parameter that characterizes the rate of conversion of turbulent-motion kinetic energy into thermal energy. Since $\bar{\varepsilon}$ determines spectral density in the inertial subrange, the value of this quantity can be used to estimate a number of practically important turbulence effects that are determined basically by wind-speed pulsations in this subrange. The quantity $\bar{\varepsilon}$ also determines diffusion processes in turbulent flow.

Two statistical characteristics – the measured values of the structure function and the spectral density of the longitudinal velocity component in the inertial subrange – were used in measuring $\bar{\varepsilon}$ on the high meteorological mast. In accordance with Stewart's data [7], the dimensionless constants in the "2/3 law" for the longitudinal structure function and the "5/3 law" for the one-dimensional longitudinal spectrum were taken equal to $C = 2$ and $C_1 = 0.5$, respectively. The analog apparatus used for these purposes permitted continuous measurement of turbulent-energy dissipation rate simultaneously on seven levels. To obtain the profiles, the results of 6 ten-minute measurements were averaged. The $\bar{\varepsilon}$-profiles obtained for the

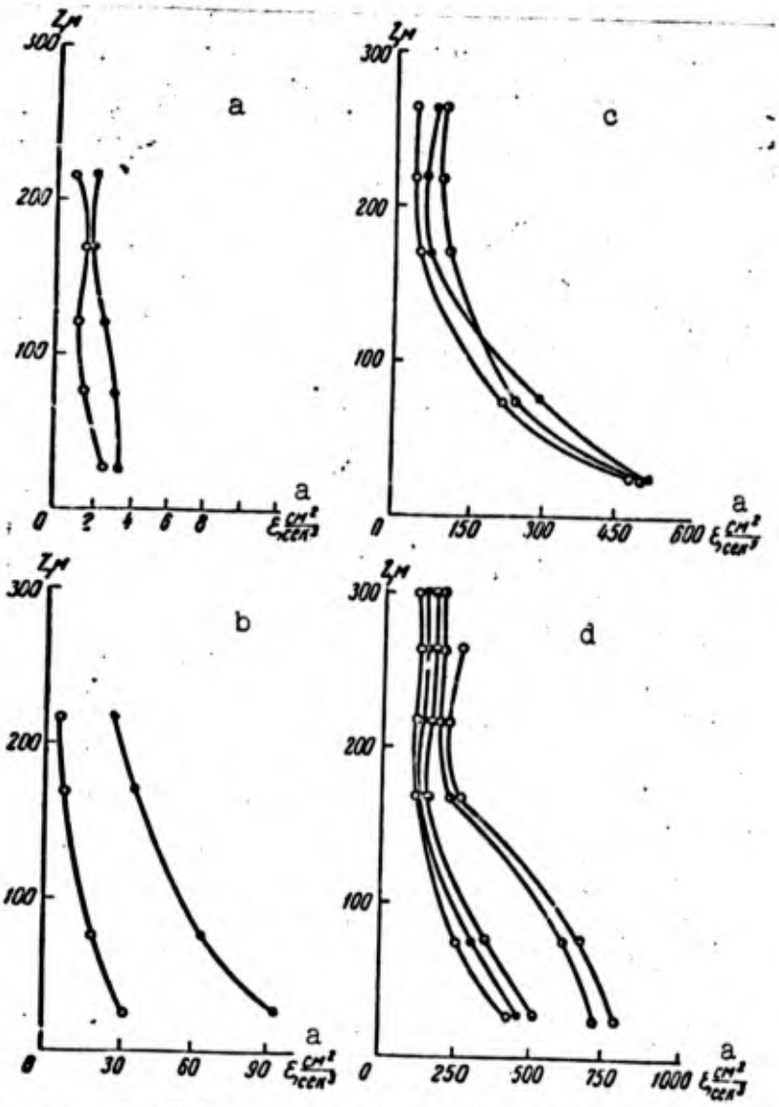

Fig. 12. Profiles of rate of turbulent energy dissipation for various stratifications, reduced to a wind speed of 5 m/s. a) weak stability; b) indifferent equilibrium; c) and d) moderate convection (the different symbols pertain to different measurement series).
KEY: (a) cm^2/s^3.

various states are shown in Fig. 12.

To exclude the effects of dynamic factors, the $\bar{\varepsilon}$-profiles were reduced to a wind speed (at the 300-m height) of 5 m/s. For this purpose, the $\bar{\varepsilon}$ were multiplied for each level by $(5/u_{300})^3$. We note that for the weak-stability states, the $\bar{\varepsilon}$-profiles are given only up to 200 m, since the stratification was different above this level. This height characterizes the thickness of the atmospheric boundary layer for this state. It exceeded 300 m for unstable states.

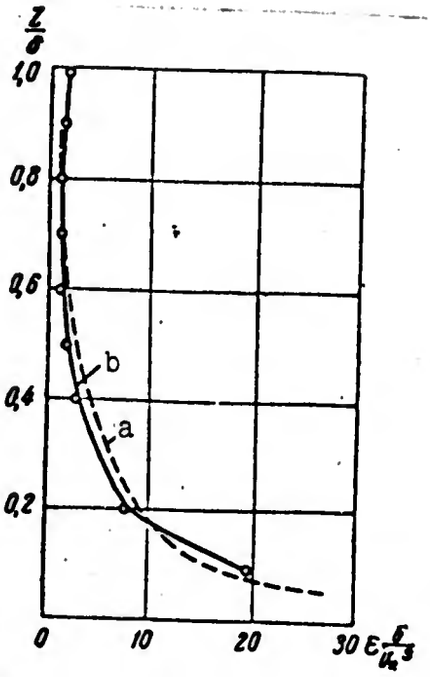

Fig. 13. Normalized profiles of turbulent-energy dissipation on a plate (a) and in the atmosphere (b).

As these diagrams show, the rate of turbulent-energy dissipation varies over a broad range for these states and diminishes with altitude. The data presented here agree with measurements made earlier on the high meteorological mast (see [3]) and with measurements of other authors.

The unstable states have a characteristic singularity in that beginning at heights of the order of 150 m, the rate of turbulent-energy dissipation stops decreasing with altitude and remains practically constant. This behavior of the turbulent energy dissipation rate can be explained on the basis of the turbulent-energy balance equation, which takes the form

$$\bar{\varepsilon} \simeq \tau \frac{\partial u}{\partial z} + \frac{g}{T} \frac{q}{c_p \rho} - \frac{\partial}{\partial z} \overline{(E'w')} \qquad (4)$$

(the nomenclature is that generally accepted). The constancy of $\bar{\varepsilon}$ may be attributed to the fact that at heights above 150 m, the first and third terms of the right member of (4) become small (beginning at these heights, the average wind speed shows practically no change with height). This leaves only the second term, which is determined by the turbulent heat flow, which shows almost no change with altitude. In this case, (4) takes the form

$$\bar{\varepsilon} \simeq \frac{g}{T} \frac{q}{\rho c_p}, \qquad (5)$$

which enables us to estimate the order of magnitude of the sum of the first and third terms in the right member of (4) below 150 m for unstable states.

For the indifferent state, the turbulent-energy dissipation-rate profiles were compared with analogous profiles measured in a wind tunnel in the boundary layer on a flat plate. It was possible to select conditions for this purpose such that the thickness δ of the atmosphere's boundary layer did not exceed 300 m. This made it possible to present the $\bar{\varepsilon}$-profile in the dimensionless coordinates z/δ and $\bar{\varepsilon}\delta/v_*^3$. The results, which appear in Fig. 13, attest to the rather good agreement of data obtained in the atmosphere and in the laboratory (at least up to a height of the order of 150 m).

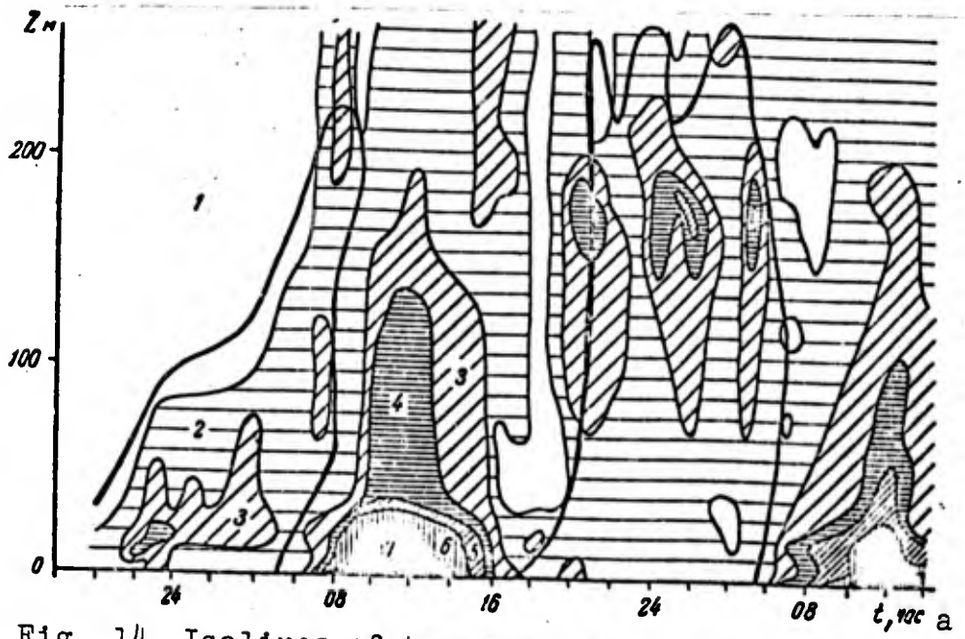

Fig. 14. Isolines of temperature-inhomogeneity intensity; the heavy line is the inversion boundary.

1 — $\sqrt{\overline{T'^2}}$ < 0.08°; 2 — 0.08—0.16°; 3 — 0.16—0.24°; 4 — 0.24—0.32°; 5 — 0.32—0.40°; 6 — 0.40—0.48°; 7 — >0.48°

KEY: (a) hours.

5. TIME CURVE OF TEMPERATURE-INHOMOGENEITY INTENSITY

The analog apparatus used in measuring turbulent energy was also used to measure the intensity of turbulent temperature inhomogeneities $\sqrt{\overline{T'^2}}$; the temperature-pulsation transducers were differential-thermocouple arrays set up at 8 levels of the meteorological mast beginning at 25 m and ending at 268 m, as well as at the 2- and 8-m levels 200 m from the mast. The frequency range of the measuring apparatus extended from 2 Hz to 2 periods/h. The data were averaged automatically over each 100 s, followed by additional 10-minute or 1-hour averaging.

The measurements were made in series lasting 40-45 h; the temperature differences between levels were registered simultaneously.

Figure 14 shows the results of one of the series of 28-30 July 1964 in the form of isolines of $\sqrt{\overline{T'^2}}$ with height and time as coordinates. This period of measurement is characterized by distinct diurnal changes in stratification: inversions at night and conspicuous daytime instability, which is supplanted after 13-15 hours by increasing cloudage of local origin, with brief light precipitation. The various types of height and time dependence of $\sqrt{\overline{T'^2}}$ for inversion, unstable stratification, and the transitional period are distinctly visible.

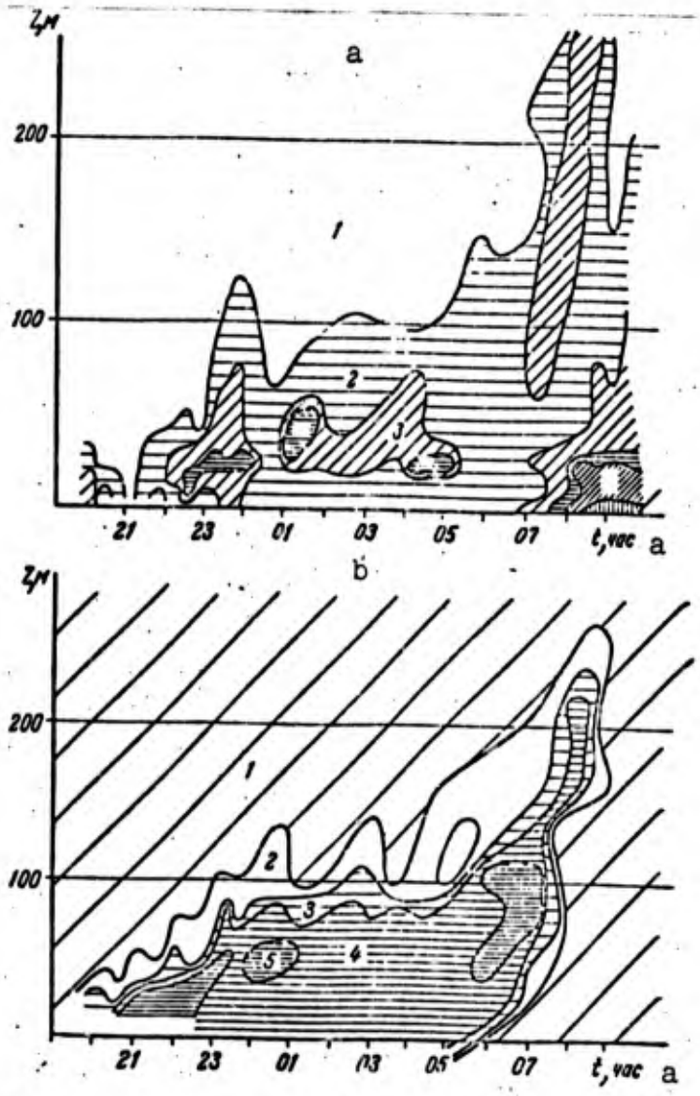

Fig. 15. Regions of equal temperature-inhomogeneity intensity (a) and equal temperature gradients $\gamma = \partial T/\partial z$ (b). The legend for a is the same as in Fig. 14; for b: 1) < 0; 2) 0-0.4°/100 m; 3) 0.4-1°/100 m; 4) 1-2.5°/100 m; 5) >2.5°/100 m. KEY: (a) hours.

During the night, the temperature-inhomogeneity intensity is distinctly related to height and the depth of the ground inversion, as is illustrated by Figs. 15 and 16, which show isolines of $\sqrt{\overline{T'^2}}$ for two nocturnal periods as obtained with averaging over a 20-minute interval and, for comparison, temperature-gradient isolines in the measured layer. Above the inversion boundary, $\sqrt{\overline{T'^2}}$ does not exceed 0.08°; its largest values, which are observed slightly below the inversion boundary, are almost an order larger (0.3-0.5°). In Fig. 15, the inversion has increased throughout the night, progressively encompassing the layer up to 200 m; the next night (Fig. 16), it covered the

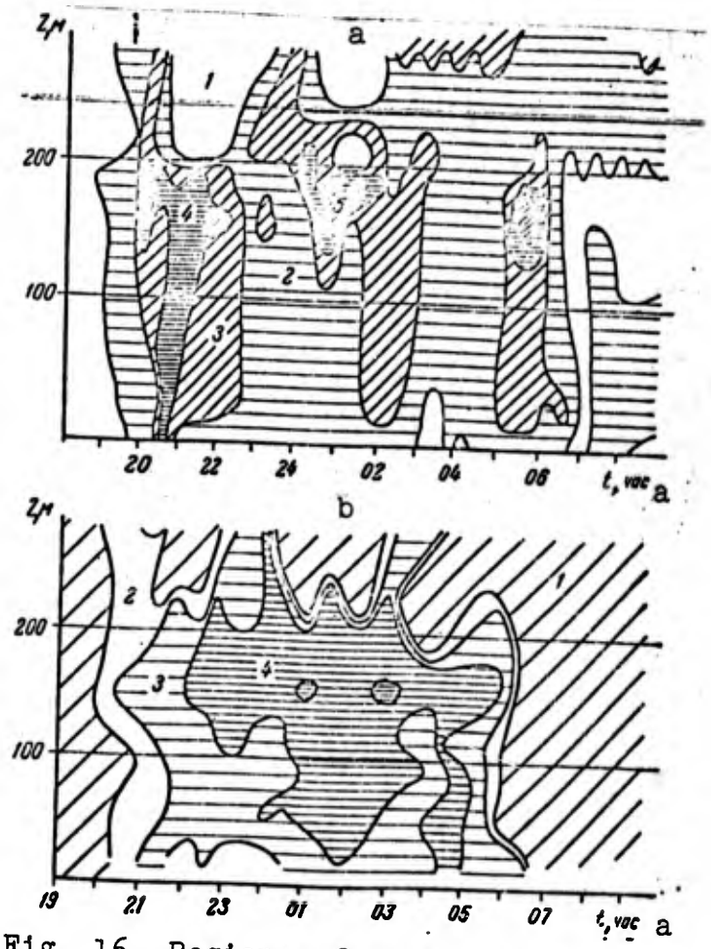

Fig. 16. Regions of equal temperature-inhomogeneity intensity (a) and equal temperature gradients $\gamma = \partial T/\partial z$ (b). Symbols same as in Fig. 15.
KEY: (a) hours.

entire layer immediately, and its upper boundary fluctuated during the night between the 200- and 300-m levels. The fluctuations of the inversion boundary in Figs. 15 and 16 are accompanied by conspicuous variations of $\sqrt{T'^2}$.

The nocturnal temperature fluctuations differ from turbulent pulsations in the usual sense. It appears that they owe their origin here to internal waves arising in the stably stratified layer, at least at weak wind-speed gradients. Typical traces of such fluctuations, obtained by aircraft measurements in both ground and elevated inversions, are given in [2, 12].

During the transition, 1-1.5 h after sunrise and the change in the sign of the temperature gradient, the temperature-inhomogeneity intensity begins to rise at low levels, and disappearance of the inversion is followed by establishment of the daytime type of intensity variation with height.

6. CHANGE IN INTENSITY OF TEMPERATURE INHOMOGENEITIES WITH HEIGHT

During the day, when stratification is unstable, $\sqrt{\overline{T'^2}}$ diminishes with height. In the ground layer, it follows from the formula of semiempirical turbulence theory

$$\sqrt{\overline{T'^2}} = \frac{cl}{E}\frac{q}{c_p\rho}\frac{\partial\theta}{\partial z}, \qquad (6)$$

where E is the turbulent energy, $q/c_p\rho$ is the turbulent heat flow divided by the specific heat and density, l is the "mixing length," and c is a dimensionless constant (see A.S. Monin [5]), that for near-indifferent stratification and in the limiting case of strong stability $\sqrt{\overline{T'^2}}$ is independent of z. In free convection, $\sqrt{\overline{T'^2}}$ is proportional to $z^{-1/3}$ (A.M. Obukhov [6]).

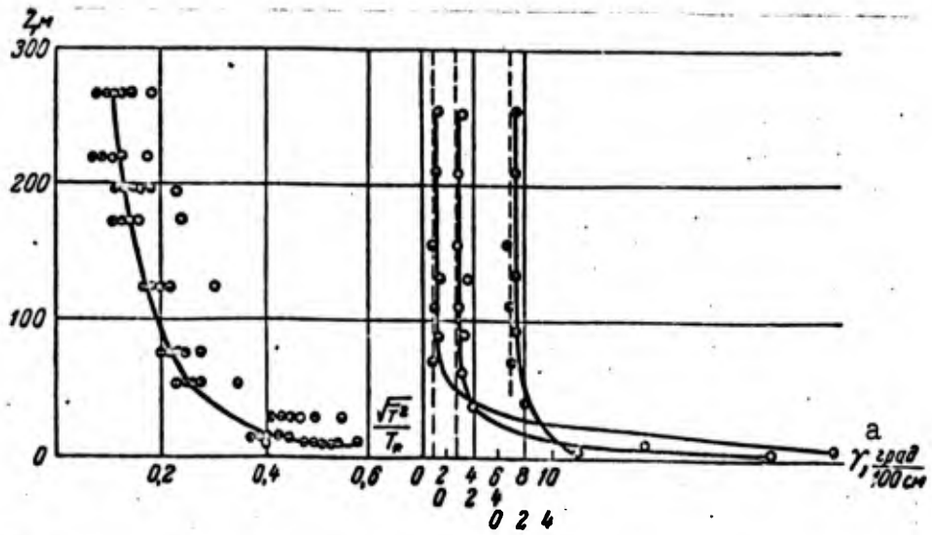

Fig. 17. Temperature-inhomogeneity intensity profiles for unstable stratification (a) and typical temperature-gradient profiles (b) (the different symbols refer to different measurement times).
KEY: (a) deg/100 cm.

It was not the purpose of this study to verify (6) for the ground layer, but the results of measurements at the 8- and 2-m levels are not contradictory to the ideas set forth above. The ratio $\sqrt{\overline{T'^2_{8m}}}/\sqrt{\overline{T'^2_{2m}}}$ was found on the average to be around unity for stable and indifferent stratification and 0.75 for unstable conditions, or somewhat higher than the theoretical value for free convection (0.63), apparently because free convection was not fully established at the heights considered.

There is no point in considering temperature-inhomogeneity intensity profiles over the entire 300-meter layer except in the daytime, when the upper layers are better coupled to the ground layer by strong mixing. The time from 10 to 14 hours was selected as an interval that approximately satisfied the stationarity condition. Figure 17 shows profiles of $\sqrt{\overline{T'^2}}$ averaged

over one-hour intervals and normalized to $T_* = -(1/\kappa v_*)(q/c_p\rho)$, where κ is the Karman constant and $v_* = (\tau/\rho)^{1/2}$ is the "friction velocity;" the same figure shows typical temperature-gradient profiles. The scatter of the points at the 25-m height is due to the unevenness of the underlying surface in the immediate vicinity of the high meteorological mast.

The heat flow was determined from the results of gradient measurements in the 1-4-m layer; since the stratification conditions under which the profiles were obtained were quite uniform and the quantity T_* is not determined very accurately for a number of reasons, the scatter of the initial data on $\sqrt{T'^2}$ was hardly reduced at all by normalization.

The phase lag at the upper levels due to the diurnal temperature variation has its effect on determination of the $\sqrt{T'^2}$ profiles. The result is that during the forenoon hours (from 9 to 12 hours), the quantity $\sqrt{T'^2}$ drops systematically with height above 100 m more rapidly than it does in the afternoon (between 12 and 14 hours). The is shown below, where we give averages of $\sqrt{T'^2}$ divided by the $\sqrt{T'^2}$ at the 2-m level for all heights separately for the 9-12 and 12-14-hour intervals:

Height, m	8	25	49	73	121	169	193	217	265
9—12 hours	0,78	0,85	0,50	0,46	0,39	0,25	0,29	0,20	0,23
12—14 hours.	0,80	0,90	0,49	0,46	0,42	0,30	0,34	0,26	0,31

References

1. N.L. Byzova and G.B. Mashkova. Otsenka zavisimosti geostroficheskogo koeffitsiyenta treniya ot stratifikatsii po nablyudeniyam v 300-metrovom sloye atmosfery (Evaluation of geostrophic coefficient of friction as a function of stratification from observations in the 300-meter layer of the atmosphere), Izv. AN SSSR, Fizika atmosfery i okeana, 1965, 1, 1209-1211.

2. V.A. Zaytsev and A.A. Ledokhovich. Termicheskaya neodnorodnost' i gorizontal'nyy gradiyent temperatury v atmosfere (Thermal inhomogeneity and the horizontal temperature gradient in the atmosphere), Trudy GGO, 1964, No. 156, 118-127.

3. V.N. Ivanov. Turbulentnaya energiya i yeye dissipatsiya (Turbulent energy and its dissipation), Izv. AN SSSR, seriya geofiz., 1963, 1405-1413.

4. A.S. Monin and V.N. Kolesnikova. O spektrakh kolebaniy meteorologicheskikh poley (Oscillation spectra of the meteorological fields), Izv. AN SSSR, Fizika atmosfery i okeana, 1965, 1, 653-669.

5. A.S. Monin. O svoystvakh simmetrii turbulentnosti v prizemnom sloye vozdukha (On the symmetry properties of turbulence in the ground layer of air), Izv. AN SSSR, Fizika atmosfery i okeana, 1965, 1, 45-54.

6. A.M. Obukhov. O strukture temperaturnogo polya i polya skorostey v usloviyakh svobodnoy konvektsii (Structure of the temperature and velocity fields under the conditions of free convection), Izv. AN SSSR, seriya geofiz., 1960, No. 9, 1392-1396.

7. R.U. Styuart. O soglasovanii imeyushchikhsya eksperimental'nykh dannykh o spektre i asimmetrii lokal'noy izotropnoy turbulentnosti (On the agreement between available experimental data on the spectrum and asymmetry of locally isotropic turbulence), Dokl. AN SSSR, 1963, 152, 324-326.

8. H.L. Grant. The Large Eddies of Turbulent Motion. Journ. of Fluid Mech., 1956, 4, 2.

9. H.A. Panofsky and R.J. Deland. One-Dimensional Spectra of Atmospheric Turbulence in the Lowest 100 meters. Advances of Geophysics, 1959, 6, 41-64 (Russian translation: G. Panovskiy and R. Delend. Odnomernyye spektry atmosfernoy turbulentnosti v pervykh 100 metrakh nad poverkhnost'yu zemli. In collection: "Atmosfernaya diffuziya i zagryazdeniye vozdukha" (Atmospheric diffusion and air pollution), Moscow, IL, 1962, 58-84.)

10. A.A. Townsend. Structure of Turbulent Shear Flow. Cambridge Univ. Press, 1956 (Russian translation: A.A. Taunsend. Struktura turbulentnogo potoka s poperechnym sdvigom. Moscow, IL, 1959).

11. Van der Hoven. Power Spectrum of Horizontal Wind Speed in the Frequency Range from 0.0007 to 900 Cycles per Hour. J. Meteorol., 1957, 14, 160-167.

12. D.R. Grant. Waves in the Inversion Layer. Meteorol. Mag., 1965, 94, 34-37.

[English Summary]

Empirical data for wind velocity and temperature fluctuations are presented. The data were obtained on the 300-metre meteorological tower of the Institute of Applied Geophysics at Obninsk.

The continuous record of wind velocity fluctuations (about 40 hrs) was used for the investigation of the low frequency subrange of the velocity spectrum. The estimated velocity spectra for 4 levels (25, 75, 150 and 300 m) are presented in Fig. 1. All the spectra contain a gap between the turbulent and mesometeorological components of the fluctuations.

The turbulent energy was evaluated for the frequency range from 0.5 cps up to 2 cph. Variances of the longitudinal wind velocity $(\overline{u'^2})^{1/2}$ were divided by the value of the wind at 300 m, u_{300}, to obtain the nondimensional turbulent intensity. Fig. 2 shows the longitudinal turbulent intensity as a function of the time of the day and the height. The profiles of turbulent intensity for different thermal stratifications (weak stability, neutral air and weak instability) are presented in Fig. 3. It shows that the turbulent intensity decreases with

the increase of stability and does not decrease with height. The profiles of the «truncated intensity» are presented in Fig. 4, where the truncated intensity is determined from the spectra with the low frequency part cut off. The great difference between the results presented in Fig. 3 and in Fig. 4 can be explained by the specific behaviour of the large—scale eddies, and it is of interest to study their structure in detail.

The space-time correlation function R_{uu} (M_0, $M_1 - M_0$, t_0, $t_1 - t_0$) of eq. (1) where $M_0 - (x_0, y_0, z_0)$ and $M_1 = (x_1, y_1, z_1)$ are used for the description of the statistical structure of large-scale eddies. The high frequency component of the fluctuations u' was filtered out by means of time averaging over 30 sec. Fig. 5 shows the vertical space correlations R_{uu} (z_0, z, t_0, 0) under conditions of weak stability. The presence of the negative values of this correlation indicates that under stable conditions the axes of the eddies have a non-zero component in the y direction.

Fig. 6 shows the time correlations R_{uu} (z_0, 0, t_0, τ) as a function of time-lag τ-$t_1 - t_0$. The corresponding integral time scales are of the order of 10—30 min. Such great time scales indicate that the eddies are strongly stretched in the longitudinal direction. Sometimes the time correlations have the form of the sum of two components with different scales (see Fig. 7).

Fig. 8 shows the space correlations R_{uu} (z_0, z, t_0, 0) under neutral conditions. These correlations have no negative range. The correlations R_{uu} (z_0, z, t_0, 0) under unstable conditions are rather large in the whole layer (see Fig. 9). Time correlations under such conditions have a negative range. The time scales are much smaller under unstable conditions than under stable conditions and the eddy structure is more isotropic in the former case.

Fig. 11 shows an example of space-time correlation.

The rate of energy dissipation ε was estimated from the measured time structure functions and time spectra using the well-known «two thirds» and «five thirds» laws with the universal coefficient recommended by Stewart [7]. Fig. 12 shows variations of ε with height under different conditions. The values of ε are multiplied by $(5/u_{300})^3$ to exclude the influence of variations of wind speed at 300 m. The rate of energy dissipation decreases with height under neutral and stable conditions but is almost constant at all heights greater than 150 m under unstable conditions. This can be explained with the help of the energy budget equation.

Fig. 14 shows the variance of temperature $(\overline{T'^2})^{1/2}$ (measured in the frequency range from 2 cps up to 2 cph) as a function of the height and the time of the day for 28—30 July 1964. The variance of temperature fluctuations at night is the greatest in the region of temperature inversion as can be seen from Figs. 15 and 16 where the isolines of temperature gradient are presented together with the magnitudes of temperature fluctuations.

Fig. 17 shows the typical profiles of $(\overline{T'^2})^{1/2}$ and of the temperature gradient under unstable conditions.

TURBULENT EXCHANGE IN THE THERMALLY STRATIFIED PLANETARY BOUNDARY LAYER OF THE ATMOSPHERE

I.M. Bobyleva
Computer Center, USSR Academy of Sciences
Siberian Division, Novosibirsk, USSR

S.S. Zilitinkevich
A.I. Voyeykov Main Geophysical Observatory,
Leningrad, USSR

D.L. Laykhtman
Leningrad Hydrometeorological Institute,
Leningrad, USSR

1. INTRODUCTION

Turbulence plays a particularly important role near the underlying surface in atmospheric motions. With increasing height, the frictional stress generated by turbulence decreases, and at a point far enough from the underlying surface it becomes negligibly small. The lowermost layer of air (with an average thickness of the order of 1 km), in which these changes take place, is known as the planetary boundary layer of the atmosphere. One of the important problems in theoretical investigation of the boundary layer is simultaneous determination of the vertical profiles of wind speed, temperature, and the turbulence characteristics for a horizontally uniform steady air flow. The basic difficulty encountered here results from nonclosure of the system of equations of the averaged motion, which makes it necessary to resort to various semiempirical hypotheses.

In the early papers devoted to this problem, the vertical distribution of the turbulent-viscosity coefficient was defined by preassigned relationships. The solution for altitude constancy of the turbulent-viscosity coefficient was first obtained by Akerblom [1]. Improved models of this coefficient's profile were proposed in the work of Rossby and Montgomery [2],

Blinova and Kibel' [3], Shvets and Yudin [4], and elsewhere.

The problem of simultaneous determination of the wind-speed and turbulent-viscosity-coefficient profiles was first examined by Monin [5] for the case of neutral stratification. To close the Reynolds equations, Monin used the balance equation of turbulence energy, expressing the coefficient of turbulent viscosity and the turbulent energy dissipation rate, with the aid of dimensional considerations, in terms of the average values of the turbulent velocity pulsation energy and a length scale characterizing the dimensions of the turbulent inhomogeneities (following Kolmogorov [6] and Obukhov [7]). This last quantity was assumed to increase linearly with height throughout the atmosphere. In the later work of Blackadar [8], Lettau [9], and Ruzin [10], which were also devoted to the case of neutral stratification, equations of the same type as in Monin's work were considered, but other expressions were used for the turbulence-scale profile.

Laykhtman [11] used elementary approximations of the turbulent-viscosity-coefficient profile to investigate the distribution of wind and temperature in the lower atmospheric layers for given external conditions. A semiempirical theory that permits analysis of the problem of turbulent exchange in a stratified atmosphere in closed form was proposed by Zilitinkevich and Laykhtman [12]. In this work, the authors obtained a solution for the relatively simple case of a ground layer (in which the effect of Coriolis forces can be regarded as negligible). The present paper considers a stratified boundary layer in which the influence of radial heat exchange is regarded as negligibly small.

2. STARTING EQUATIONS

Following basically the semiempirical theory set forth in [12], we shall write the system of equations of turbulent motion in the following form for the conditions considered:

$$\lambda v - \frac{1}{\rho}\frac{\partial p}{\partial x} + \frac{d}{dz}k\frac{du}{dz} = 0, \quad -\lambda u - \frac{1}{\rho}\frac{\partial p}{\partial y} + \frac{d}{dz}k\frac{dv}{dz} = 0, \tag{1}$$

$$\alpha_T \frac{d}{dz}k\frac{d\theta}{dz} = 0, \tag{2}$$

$$k\left[\left(\frac{du}{dz}\right)^2 + \left(\frac{dv}{dz}\right)^2\right] - \alpha_T \frac{g}{T}k\frac{d\theta}{dz} + \alpha_b \frac{d}{dz}k\frac{db}{dz} = \varepsilon, \tag{3}$$

$$k = b^{1/2}l, \qquad \varepsilon = c\frac{b^{3/2}}{l}, \tag{4}$$

$$l = -\varkappa\frac{\Psi}{\frac{d\Psi}{dz}}, \quad \Psi = \left(\frac{du}{dz}\right)^2 + \left(\frac{dv}{dz}\right)^2 - \alpha_T\frac{g}{T}\frac{d\theta}{dz} + \frac{\alpha_b}{k}\frac{d}{dz}k\frac{db}{dz}. \tag{5}$$

Here x, y, and z are Cartesian coordinates (z is height); the unknowns are: u and v, the horizontal components of mean wind speed; θ, the potential temperature; k, the coefficient of turbulent viscosity; ε, the mean rate of dissipation of turbulent energy as heat; b and l, the mean values of kinetic energy and the spatial scale of the pulsations. The remaining quantities, which are assumed constant, have the following sense: λ, the Coriolis parameter; ρ, the density of the air; $\partial p/\partial x$ and $\partial p/\partial y$, the components of the horizontal pressure gradient; g, the

acceleration of gravity; T, the characteristic value of absolute temperature in the layer under consideration; α_T, α_b, c and $\tilde{\kappa}$, dimensionless constants whose empirical values are given in [12]. We give improved values of these constants, which have been calculated as in [12], by using more accurate experimental data [13, 14]: $\alpha_T \approx 1$; $\alpha_b \approx 0.73$; $c \approx 0.46 \cdot 10^{-1}$; $\tilde{\kappa} \approx 0.37$. As is shown in [12], the quantity $\tilde{\kappa}$ is related to Karman's constant $\kappa \approx 0.4$[1] by the relationship $\tilde{\kappa} = 2\kappa c^{1/4}$. Wherever this formula is used below, we shall substitute for $\tilde{\kappa}$ the corresponding combination containing the more familiar constant κ.

We note that Eq. (5), which determines the average turbulence scale, differs from that proposed in [12] in that it takes account of the veering (backing) of the wind (which was not required for analysis of the ground layer) and has the term $\frac{\alpha_b}{k}\frac{d}{dz}k\frac{d\psi}{dz}$ in the expression for the "characteristic function" Ψ. The point is that the specific calculations in [12] were performed without consideration of the turbulent-energy diffusion effect (i.e., for $\alpha_b = 0$). In the present study, where this effect is taken into consideration, it is postulated that its role in shaping the turbulent-vortex scales can be reflected by the modification indicated above in the expression for the function Ψ.

In the form of (2), the heat flux equation is greatly simplified, primarily because it does not have the term describing the radiative heat-transfer effect. It is because of this that the present study does not raise the question of investigating the vertical temperature distribution in the boundary layer. Our object here is elementary correction of the wind-speed distribution and the main turbulence characteristics for the effect of thermal stratification. Considering this formulation of the problem, it is convenient to assume that the vertical turbulent heat flow q, which in our case is found to be constant over height by virtue of (2), is given:

$$q = -\alpha_T c_p \rho k \frac{d\theta}{dz} = \text{const} \qquad (6)$$

(c_p is the heat capacity of air at constant pressure).

Despite the fact that Relationship (6) is usually violated in the real atmosphere above one hundred meters (see [15, 16] and Fig. 6 on page 20), it may apparently be assumed that the errors in determination of the wind profile that are incurred by using it will be small. This is because the wind is, as a rule, very close to geostrophic at levels where q becomes substantially variable. It is also natural to assume that the errors in determination of such characteristics as the turbulent viscosity coefficient, the rate of dissipation of turbulent energy as heat, etc., will also be small at low levels, since the heat flux here is effectively constant.

[1] See page 69 for footnote.

3. BOUNDARY CONDITIONS

Let us orient the x-axis in the direction of the ground wind. We shall use the nomenclature

$$\frac{1}{\lambda\rho}\frac{\partial p}{\partial x} = G\sin\alpha, \qquad -\frac{1}{\lambda\rho}\frac{\partial p}{\partial y} = G\cos\alpha, \tag{7}$$

where G is the absolute value of geostrophic wind speed, and α is the angle between this speed and the x-axis (and is equal to the full rotation angle of the wind in the boundary layer). As usual, the boundary conditions for the wind-speed components will be written

$$u \to 0, \quad v \to 0 \quad \text{as } z \to z_0, \tag{8}$$

$$u \to G\cos\alpha, \quad v \to G\sin\alpha \quad \text{as } z \to \infty. \tag{9}$$

Here z_0 is the aerodynamic roughness of the underlying surface.

Let us introduce the friction velocity v_*, which is defined by the equality $v_*^2 = \lim_{z \to z_0} k\frac{du}{dz}$.[2] To obtain the lower boundary condition that must be satisfied by the mean turbulence energy b, we shall utilize the fact that the absolute value of the diffusion energy flux $\alpha_b k(db/dz)$ cannot increase without limit as z decreases. Applying (1)-(5), it is easy to show (cf. [12]) that this implies

$$b \to c^{-1/3}v_*^2 \quad \text{as } z \to z_0. \tag{10}$$

Under conditions of stable and neutral stratification ($z \leq 0$), the quantity b should vanish as $z \to \infty$, since the wind shear that results from sticking of the air to the underlying surface is then the only cause of turbulence. For unstable stratification in this case of altitude-constant heat flow, the turbulent exchange should correspond to the conditions of free convection at great enough altitudes. According to [17, 18], the expression $b = C\left(\frac{g}{T}\frac{q}{c_p\rho}z\right)^{2/3}$, where C_0 is a dimensionless universal constant, will obtain here for b. The value of the constant is readily expressed in terms of the quantities c, κ and α_b if we use Eqs. (2)-(5).[3] Omitting the bookkeeping, we write the results in the form

$$b|_{z\to\infty} \to \begin{cases} 0 \text{ for } q < 0, \\ \kappa^{2/3}c^{-1/3}\left(\frac{2}{3} - \frac{\kappa^2\alpha_b}{c^{1/3}}\right)^{-2/3}\left(\frac{g}{T}\frac{q}{c_p\rho}z\right)^{2/3} \quad \text{for } q > 0. \end{cases} \tag{11}$$

Thus, we have formulated the required boundary conditions. The problem now consists in determining profiles of the quantities u, v, k, ε, b and ℓ, with the "external parameters" G, z,

[2, 3] See page 69 for footnotes.

λ, g/T and $q/c_p\rho$ regarded as given (the parameters v_* and α are subject to determination).

4. THE TRANSITION TO UNIVERSAL RELATIONSHIPS

Let us introduce the new variables

$$\eta = k\frac{du}{dz}, \qquad \sigma = k\frac{dv}{dz}. \tag{12}$$

Applying (1), (7), and (12), we find

$$v - G\sin\alpha = -\frac{1}{\lambda}\frac{d\eta}{dz}, \qquad u - G\cos\alpha = \frac{1}{\lambda}\frac{d\sigma}{dz}. \tag{13}$$

It is evident from this that it is sufficient to know α and the functions η and σ to determine the profiles of u and v. Differentiating (13), we obtain the following equations that must be satisfied by these functions:

$$\frac{d^2\eta}{dz^2} + \frac{\lambda}{k}\sigma = 0, \qquad \frac{d^2\sigma}{dz^2} - \frac{\lambda}{k}\eta = 0. \tag{14}$$

The boundary conditions for the quantities η and σ can be obtained from (8) and (9) by applying (13). But we shall dispense temporarily with these relationships and write the required conditions in the following form, considering the orientation selected for the coordinate axes:

$$\eta \to v_*^2,\ \sigma \to 0 \quad \text{as } z \to z_0, \tag{15}$$

$$\eta \to 0,\ \sigma \to 0 \quad \text{as } z \to \infty. \tag{16}$$

Since v_* and α are unknown, Relationships (15) are trivial identities. On the other hand, Relationships (16) are equivalent in this problem to Conditions (9).

Let us introduce the parameter L_1, which has the dimensions of length, and the dimensionless parameter μ by the formulas

$$L_1 = \frac{\varkappa v_*}{\lambda}, \qquad \mu = -\varkappa^3\frac{g}{T}\frac{\frac{q}{c_p\rho}}{\lambda v_*^2}. \tag{17}$$

We further introduce the dimensionless variables

$$z_n = \frac{z}{L_1}, \quad \eta_n = \frac{\eta}{v_*^2}, \quad \sigma_n = \frac{\sigma}{v_*^2}, \quad k_n = \frac{k}{\varkappa v_* L_1},$$

$$\varepsilon_n = \frac{\varkappa L_1}{v_*^3}\varepsilon, \quad b_n = \frac{c^{1/2}}{v_*^2}b, \quad l_n = \frac{l}{\varkappa c^{1/4} L_1}. \tag{18}$$

The system (3)-(5), (10), (11), (14)-(16) then assumes the form[4]:

$$\frac{d^2\eta_n}{dz_n^2} + \frac{\sigma_n}{k_n} = 0, \qquad \frac{d^2\sigma_n}{dz_n^2} - \frac{\eta_n}{k_n} = 0. \tag{19}$$

[4]See page 69 for footnote.

$$\frac{\eta_n^2+\sigma_n^2}{k_n}-\mu+\beta\frac{d}{dz_n}k_n\frac{db_n}{dz_n}=\varepsilon_n,$$

$$k_n=b_n^{1/2}l_n,\quad \varepsilon_n=\frac{b_n^2}{k_n},\quad l_n=-\left(\frac{d}{dz_n}\ln\frac{b_n}{k_n}\right)^{-1}, \tag{20}$$

$$\eta_n|_{z_n\to 0}\to 1,\quad \sigma_n|_{z_n\to 0}\to 0,\quad \eta_n|_{z_n\to\infty}\to 0,\quad \sigma_n|_{z_n\to\infty}\to 0, \tag{21}$$

$$b_n|_{z_n\to 0}\to 1,\quad b_n|_{z_n\to\infty}\to\begin{cases}0 & \text{for } \mu>0,\\ \left(\frac{2}{3}-3\right)^{-1/3}\mu^{1/2}z_n^{1/2} & \text{for } \mu<0.\end{cases} \tag{22}$$

(23)

Here β is a universal numerical constant, $\beta=\frac{\varkappa^2\alpha_b}{c^{1/3}}$.

The solution of the boundary-value problem (19)-(23) is expressed in the form of the following set of universal functions of the variable z_n, which depend on the parameter μ:

$$\eta_n=H_\mu(z_n),\quad \sigma_n=\Sigma_\mu(z_n),\quad k_n=K_\mu(z_n),$$
$$\varepsilon_n=E_\mu(z_n),\quad b_n=B_\mu(z_n),\quad l_n=\Lambda_\mu(z_n). \tag{24}$$

We shall now indicate a method of calculating the wind-speed components. Let us introduce, in addition, the dimensionless variables

$$u_n=\frac{\varkappa}{v_*}u,\quad v_n=\frac{\varkappa}{v_*}v. \tag{25}$$

Applying (13), (18), (25), we obtain

$$u_n-\frac{\varkappa G}{v_*}\cos\alpha=\frac{d\sigma_n}{dz_n}=F_\mu^{(1)}(z_n),$$
$$v_n-\frac{\varkappa G}{v_*}\sin\alpha=-\frac{d\eta_n}{dz_n}=F_\mu^{(2)}(z_n). \tag{26}$$

To complete formulation of the computational problem, we have only to indicate the recipe for determining the parameters v_* and α from the given G, z_0, λ, g/T and $q/c_p\rho$. As a dimensional analysis indicates, this procedure reduces to finding two universal functions that express the geostrophic coefficient of friction v_*/G and the boundary-layer wind total rotation angle α as functions of the dimensionless parameters[5]

$$\mathrm{Ro}=\frac{G}{\lambda z_0},\qquad M=-\frac{q}{T}\frac{\frac{q}{c_p\rho}}{\lambda G^2}. \tag{27}$$

To determine the form of the relationships sought, let us return to Conditions (8). Applying (13), converting to dimensionless variables, and then squaring and adding the resulting relationships, we find

$$r=\varkappa^2\mathrm{Ro}=\frac{1}{z_{0n}}\left|\sqrt{\left(\frac{d\eta_n}{dz_n}\right)^2+\left(\frac{d\sigma_n}{dz_n}\right)^2}\right|_{z_n=z_{0n}}=\Phi_\mu(z_{0n}). \tag{28}$$

Here r, the new dimensionless characteristic of the condition studied, is more convenient from the standpoint of numerical

[5]See page 69 for footnote.

solution than Ro; Φ_μ is a universal function of the variable $z_{0n} = z/L_1$, and depends on the parameter μ. Denoting the reciprocal function of Φ_μ by Φ_μ^*, we obtain from (28)

$$\frac{\tau_0}{\kappa G} = \frac{1}{r\,\Phi_\mu^*(r)} = \chi_\mu(r). \tag{29}$$

Let us now divide the first relationship of (8), transformed with (13), term by term by the second. Writing the result in dimensionless form, we find

$$-\alpha = \operatorname{arctg} \left. \frac{\frac{d\eta_n}{dz_n}}{\frac{d\sigma_n}{dz_n}} \right|_{z_n = z_{0n}} = \Omega_\mu(z_{0n}) = \Omega_\mu(\Phi_\mu^*(r)) = \zeta_\mu(r). \tag{30}$$

Here Ω_μ is a universal function of the argument z_{0n} and depends on the parameter μ; χ_μ and ζ_μ are universal functions of the argument $\underline{r}$ and also depend on the same parameter.

The relation between the values of parameters μ, M, and $\underline{r}$ (or Ro) is obtained by combining (17), (27), and (29) in the form

$$M = \mu\,[\chi_\mu(r)]^2 = \omega_\mu(r), \tag{31}$$

where ω_μ is one more universal function of the argument $\underline{r}$ that depends on the parameter μ.

5. RESULTS OF NUMERICAL SOLUTION

The problem formulated above was solved numberically with an M-20 electronic computer. The calculations were carried out for μ of -100, -10, 0, +10, +100 with $\beta = 0.54$ (which corresponds to the values indicated above for the constants $\underline{c}$, α_b and κ). The solution was constructed by breaking up the entire system into Subsystems (19), (22) and (20), (21), (23), using iterations in k_n. The initial relationship was in most cases the linear one $k_n = z_n$. Then problem (19), (22) was solved by matrix factoring for each of the $k_n(z_n)$ relationships obtained in the preceding step. The relationships $\eta_n(z_n)$ and $\sigma_n(z_n)$ determined in this manner were substituted into Subsystem (20), (21), (23), whose solution was found by the exclusion method. This procedure was repeated until the maximum deviation of the resulting function $k_n(z_n)$ from the preceding one satisfied some predetermined accuracy criterion. The sensitivity of the solution to displacements of the lower and upper limits of variation of z_n was checked by numerical experiments. The result was confirmation of the admissibility of replacing (15) by (22); the critical values of the upper z_n limit beyond which a further increase had no influence on the form of the solution were also found for each μ.

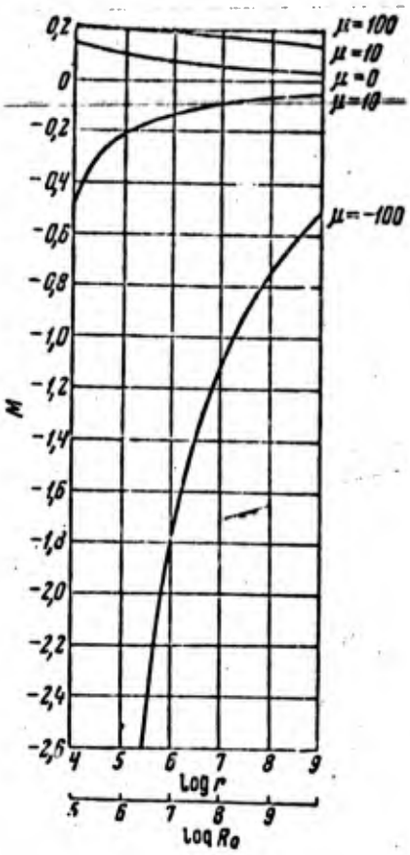

Fig. 1. Alignment chart for determination of parameter μ from given Ro and M (the curves are μ = = const isolines).

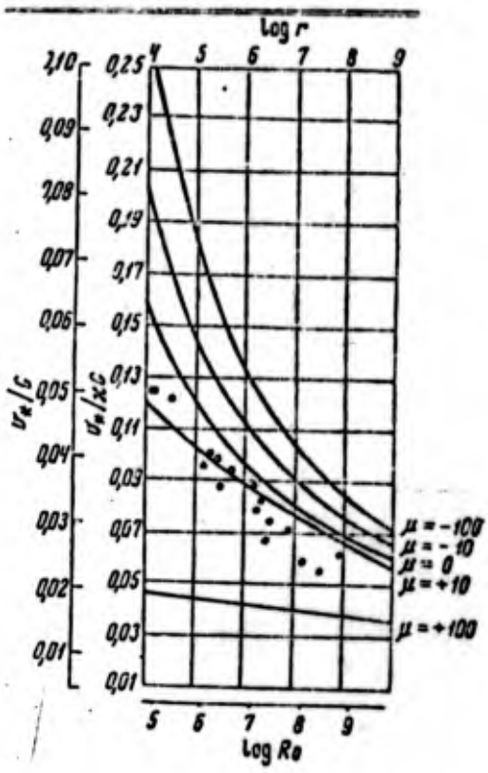

Fig. 2. Geostrophic coefficient of friction v_*/G as a function of Rossby number Ro for various values of parameter μ.

Figures 1-3 show diagrams of the universal relationships $M = \omega_\mu(r)$, $v_*/\kappa G = \chi_\mu(r)$ and $-\alpha = \zeta_\mu(r)$[6] for the above five values of the parameter μ. The scale of the variable Ro is given in all cases for further convenience, and Fig. 2 also has a scale for v_*/G. In constructing these supplementary scales, the constant κ was taken equal to 0.4. These relationships enable us to determine μ, v_* and α from given "external parameters" Ro and M. The points plotted in Figs. 2 and 3 represent experimental determinations, borrowed from Blackadar's paper [8], for the geostrophic coefficient of friction and the wind total rotation angle in the boundary layer. The stability conditions under which these data were obtained are assumed to be close to neutral, but are not precisely defined. As the figures show, the values given for both v_*/G and α agree satisfactorily with theoretical predictions if we regard them as pertaining to weak-stability conditions.

[6]See page 69 for footnote.

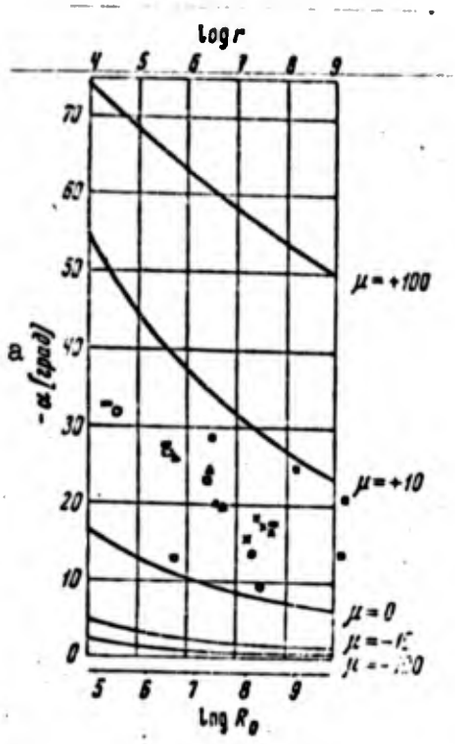

Fig. 3. Angle α of full wind rotation in the atmospheric boundary layer as a function of Rossby number Ro for various values of parameter μ.
KEY: (a) degrees.

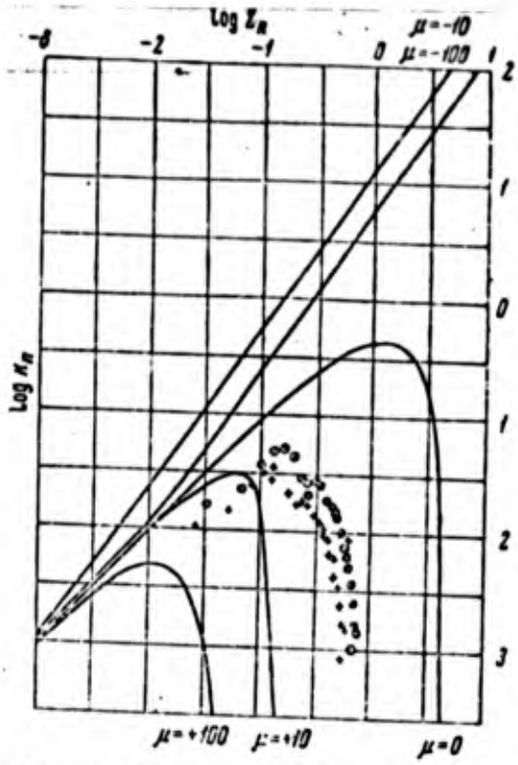

Fig. 4. Universal profiles of turbulent viscosity coefficient $k_n = K_\mu(z_n)$.

The dimensionless profiles of the turbulent viscosity coefficient $k_n = K_\mu(z_n)$ and the rate of dissipation of turbulent energy as heat $\varepsilon_n = E_\mu(z_n)$ are shown in Figs. 4 and 5 for various μ.[7] The empirical data of Lettau and Hoeber [19], which were obtained in two series of special observations (different symbols are used for the data of each series) are shown, reduced to dimensionless form, in the first of these figures. The experimental data given in Fig. 5 for the rate of turbulent energy dissipation were taken from Ball's paper [20].[8] These data represent a comprehensive summary of the measurement results obtained by various authors. The considerable scatter observed here can be explained, among other things, by the stratification effect. We note that the data of [20] (like those of [8] and [19]) group basically around the theoretical curves corresponding to weak-stability states, which are most characteristic for the planetary boundary layer of the atmosphere.

[7,8] See page 69 for footnotes.

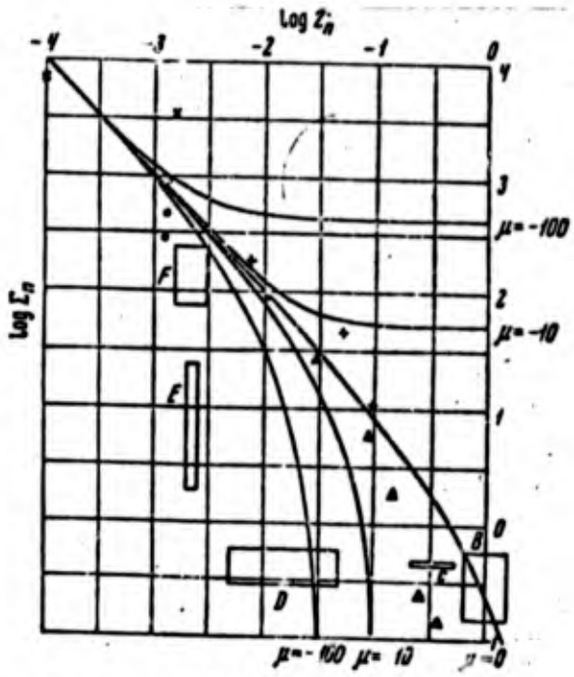

Fig. 5. Universal profiles of turbulent energy dissipation rate $\varepsilon_n = E_\mu(z_n)$.

The universal functions $F_\mu^{(1)}(z_n)$ and $F_\mu^{(2)}(z_n)$, which describe the wind profile in the boundary layer, are shown in Figs. 6a and b. Of a certain interest here is the "jet stream" obtained theoretically for heights of the order of 100-200 m in temperature inversions ($\mu > 0$). As we see from the figures, this effect is particularly significant for $\mu = +100$, when the "jet stream" is found to be localized in a layer a few tens of meters thick, with the maximum velocity about one and a half times greater than the geostrophic velocity.

In summarizing, we note that universal relationships similar to those given in Figs. 1-6, given a sufficiently complete set of values of the parameter μ, yield, in principle, an exhaustive description of the elementary statistical characteristics of turbulent exchange in the atmosphere's planetary boundary layer. It is the authors' view that the pressing problem for further study of the boundary layer consists in fitting and organizing the experimental data for detailed verification of the theory.

The authors thank G.I. Marchuk for helpful discussion.

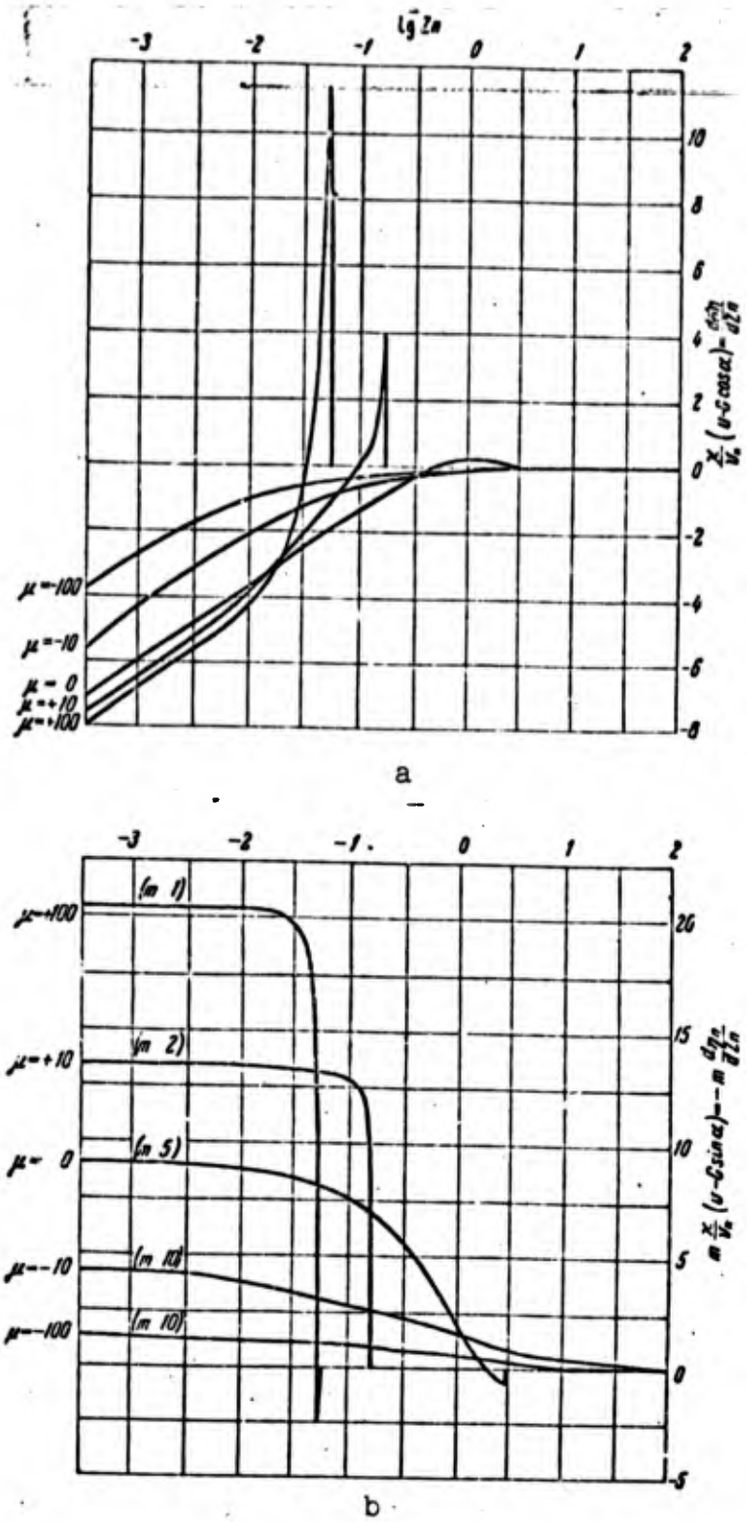

Fig. 6. Universal wind profiles in atmosphere boundary layer. a) component longitudinal with respect to ground wind; b) component transverse to ground wind.

References

1. F. Akerblom. Recherches sur les courants les plus bas de l'atmosphere au-dessus du Paris (Studies of the lowest-level currents in the atmosphere over Paris), Nova Acta Reg. Soc. Sci. Upsala, 1908, Ser. 4, 2, No. 2, 1-45.

2. C.G. Rossby and R.B. Montgomery, The Layer of Frictional Influence in Wind and Ocean Currents. Pap. Phys. Ocean. Meteorol., 1935, 3, No. 3,1-101.

3. B.A. Izvekov and N.Ye. Kochin (Ed.). Dinamicheskaya meteorologiya (Dynamic meteorology), Chapter 8, Gidrometeoizdat, 1937, pp. 28-36.

4. M.Ye. Shvets and M.I. Yudin. Statsionarnaya model' raspredeleniya vetra s vysotoy v turbulentnoy atmosfere (A stationary model of wind distribution over altitude in a turbulent atmosphere), Trudy Glavnoy geofiz. obs., 1940, No. 31, 42-52.

5. A.S. Monin. Dinamicheskaya turbulentnost' v atmosfere (Dynamic turbulence in the atmosphere), Izv. AN SSSR, seriya geogr. i geofiz., 1950, 14, No. 3, 232-254.

6. A.N. Kolmogorov. Uravneniya turbulentnogo dvizheniya neszhimayemoy zhidkosti (Equations of turbulent motion of an incompressible fluid), Izv. AN SSSR, seriya fiz., 1942, 6, No. 1-2, 56-58.

7. A.M. Obukhov. Turbulentnost' v temperaturno-neodnorodnoy atmosfere (Turbulence in a nonuniform-temperature atmosphere), Trudy In-ta teor. geofiz. AN SSSR, 1946, 1, 95-115.

8. A.K. Blackadar. The Distribution of Wind and Turbulent Exchange in a Neutral Atmosphere. J. Geophys. Res., 1962, 67, No. 8, 3095-3102.

9. H.H. Lettau. Theoretical Wind Spirals in the Boundary Layer of a Barotropic-Atmosphere. Beitr. Phys. Atmosph., 1962, 35, No. 3/4, 195-212.

10. M.I. Ruzin. Vertikal'nyy profil' koeffitsiyenta turbulentnosti v pogranichnom sloye atmosfery (Vertical profile of turbulence coefficient in the boundary layer of the atmosphere), Trudy Vses. nauchnogo meteor. soveshch. (Transactions of All-Union Scientific Meteorological Conference), Vol. 7, Gidrometeoizdat, 1963, pp. 63-72.

11. D.L. Laykhtman. Fizika pogranichnogo sloya atmosfery (Physics of the atmosphere's boundary layer), Chapter 2, Gidrometeoizdat, 1961, pp. 41-89.

12. S.S. Zilitinkevich and D.L. Laykhtman. Turbulentnyy rezhim v prizemnom sloye atmosfery (Turbulent exchange in the

ground layer of the atmosphere), Izv. AN SSSR, Fizika atmosfery i okeana, 1965, 1, No. 2, 150-156.

13. J. Laufer. The Structure of Turbulence in Fully Developed Pipe Flow. NACA Tech. Rep., 1954, No. 1174.

14. P.S. Klebanoff. Characteristics of Turbulence in a Boundary Layer with Zero Pressure Gradient. NACA Tech. Notes, 1954, No. 3178.

15. W.P. Elliot. The Height Variation of Vertical Heat Flux near the Ground. Quart. J. Roy. Meteorol. Soc., 1964, 90, No. 385, 260-265.

16. J.W. Telford and J. Warner. Fluxes of Heat and Vapor in the Lower Atmosphere Derived from Aircraft Observations. J. Atmosph. Sci., 1964, 21, No. 5, 539-548.

17. A.S. Monin and A.M. Obukhov. Osnovnyye zakonomernosti turbulentnogo peremeshivaniya v prizemnom sloye atmosfery (Basic relationships in turbulent mixing in the ground layer of the atmosphere), Trudy Geofiz. in-ta AN SSSR, 1954, No. 24. (151), 163-187.

18. A.M. Obukhov. O strukture temperaturnogo polya i polya skorostey v usloviyakh svobodnoy konvektsii (On the structure of the temperature and velocity fields under free-convection conditions), Izv. AN SSSR, seriya geofiz., 1960, No. 9, 1392-1396.

19. H.H. Lettau and H. Hoeber. Uber die Bestimmung der Höhen-Verteilung von Schubspannung und Austauschkoeffizient in der atmospherischen Reibungsschicht (Determination of altitude distribution of shear stress and coefficient of exchange in the friction layer of the atmosphere), Beitr. Phys. Atmosph., 1964, 37, No. 2, 105-118.

20. F.K. Ball. Viscous dissipation in the Atmosphere. J. Meteorol., 1961, 18, No. 4, 553-557.

[English summary]

One of the important problems of theoretical research of the atmospheric planetary boundary layer is the determination of consistent vertical profiles of wind speed, temperature, and turbulence characteristics for horizontally homogeneous stationary air flow. The main difficulty is connected with the fact that the mean motion equations are indeterminate. This leads to the necessity of using some semi-empirical hypothesis for closure of the equations.

For the case of a neutral stratification the problem in question was first considered by Monin [5]. For closure of the Reynolds equations Monin (following Kolmogorov and Obukhov) used the equation for the turbulent energy budget. In this equation he expressed the exchange coefficient for momentum and the rate of turbulent energy dissipation in terms of the mean energy and mixing-lenght (i. e., characteristic length-scale) of the turbulent eddies. The mixing-length was assumed by Monin to be linearly increasing with height in the whole atmosphere. Later Blackadar [8] and Lettau [9] made some attempts to use more realistic profiles of the mixing-length. Their approximation of the mixing-length profile provided a finite upper bound for this length at high levels.

This paper considers the case of the diabatic planetary boundary layer. Under these conditions the buoyancy term plays an important role in the equation for the budget of turbulent energy. The treatment of the problem in this paper differs from those mentioned above in that for the definition of the mixing-length a special hypothesis is proposed, which is the generalization of the well-known von Karman hypothesis of local similarity. This gives the opportunity of expressing the mixing-length by means of local characteristics of average motion.

Following the semi-empirical theory the system of turbulent motion equations can then be written as (1)—(5). In these equations u and v are the horizontal components of mean wind, θ is the potential temperature, k is the kinematic exchange coefficient for momentum, ε is the mean rate of turbulent energy dissipation, and b and l are the mean values of turbulent energy and mixing-length of the eddy. The other parameters are assumed to be constant: λ is the Coriolis parameter, ρ is the air density, $\partial p/\partial x$ and $\partial p/\partial y$ are the components of horizontal pressure gradient, g is the acceleration of gravity, T is the typical temperature of the boundary layer, α_T, α_b, c and $\tilde{\varkappa}$ are nondimensional constants. It is convenient to suppose that the heat flux q is independent of height (see eq. (6)). If the x-axis coincides with the surface wind direction, one can write eq. (7) where G is the geostrophic wind speed and α is the angle between the geostrophic wind direction and the x-axis. The boundary conditions for the wind speed components are usually represented as (8), (9). Introducing friction velocity v_* as $v_*^2 = \lim_{z \to z_0} k \frac{du}{dz}$ and using the equations (1) — (5) one can derive eq. (10) where z_0 stands for the aerodynamic surface roughness. In cases of stable and neutral stratification (when $q \leqslant 0$) b must approach zero when $z \to \infty$. Under conditions of unstable stratification $b = C_0 \left(\frac{g}{T} \frac{q}{c_p \rho} z\right)^{1/3}$ at high levels according to Monin and Oboukhov [17]. C_0 can be expressed in terms of c, $\tilde{\varkappa}$ and α_b giving (11). Thus, the necessary boundary conditions (8)—(11) are formulated. Our problem now is to define the profiles of u, v, k, ε, b and l assuming that the «exterior parameters» G, z_0, λ, g/T and $q/c_p \rho$ are given.

Let (12), (18) be new variables. Introducing two nondimensional parameters μ and L_1 by (17) one can obtain a closed system of equations (19) — (23). The solution of this boundary problem is expressed by the set of universal functions (24) of the variable $z_n = z/L_1$, which depend on the parameter μ.

The formulated problem was solved numerically by means of the digital computer M-20. The calculations were carried out for the following values of μ: -100, $-10{,}0$, $+10$, $+100$. In Figs. 1, 2, 3 the universal functions (31), (29) and (30) respectively are presented for the five above — mentioned values of μ. These functions give the opportunity to define μ, v_* and α if the «exterior parameters» (27) are given. The experimental and computed values of the geostrophic drag coefficient and the angle α in the boundary layer are plotted in Figs. 2 and 3.

The nondimensional profiles of the exchange coefficient for momentum and for the rate of turbulent energy dissipation are given in Figs. 4,5 for different μ.

The universal functions (26) which describe the wind profile are presented in Fig. 6, *а*, *б*.

The theoretically obtained «jet stream» at altitudes of about 100—200 m for the case of a temperature inversions ($\mu > 0$) is of some interest. The figures show that this effect is considerable when $\mu = +100$. The thickness of the «jet stream» turns out to be several dozen metres and the maximum velocity turns out to be 1.5 times as large as the geostrophic value.

Footnotes

Manuscript page

56 [1]Here the Karman coefficient is defined as the numerical coefficient in the familiar formula for the velocity profile in a logarithmic boundary layer, $u = (v_*/\kappa) \ln z + \text{const}$, where v_* is the friction velocity.

57 [2]In the coordinate system adopted, $\lim_{z \to z_*} k \frac{du}{dz} = 0$. Hence this definition is the same as the usual one.

57 [3]A similar procedure is used in [12] to determine another constant.

58 [4]The lower boundary conditions for η_n, σ_n and b_n in Formulas (22) and (23) are written for $z_n = 0$ instead of $z_n = z_0/L_1$. This simplification was first applied in [5] for neutral-stratification conditions. In the present study, the admissibility of this simplification was checked by numerical trials with the quantity z_0/L_1 varied; the results showed that for values of the roughness parameter that are really of interest ($0 < z_0 < 1$ m), its magnitude has practically no influence on the solution of Problems (19)-(23).

59 [5]The quantity Ro is sometimes known as the Rossby parameter; the dimensionless number M is an external stratification parameter (unlike the Richardson number, which is an internal or local stratification parameter).

61 [6]Negative values of the angle α correspond to veering of the wind in the Northern Hemisphere.

62 [7]To the extent that the profiles of $\underline{k}$ and ε have been established, determination of the $\underline{b}$ and ℓ profiles reduces to elementary calculations by Formulas (4) or (21).

Manu-
script
page

62 [8]In reducing the data of [20] to dimensionless form, we used $v_* = 0.4$ m/s and $\phi = 50°$ as characteristic values of the friction velocity and geographic latitude for normalization of $\underline{z}$ and ε by Formulas (18).